

THESIS

VARIABLE FRESH SNOW ALBEDO: HOW SNOWPACK AND SUB-NIVEAN  
PROPERTIES INFLUENCE FRESH SNOW REFLECTANCE

Submitted by

Danielle C. Reimanis

Department of Ecosystem Science and Sustainability

In partial fulfillment of the requirements

For the Degree of Master of Science

Colorado State University

Fort Collins, Colorado

Fall 2021

Master's Committee:

Advisor: Steven Fassnacht

Gregory Butters  
Daniel McGrath

Copyright by Danielle Catherine Reimanis 2021

All Rights Reserved

## ABSTRACT

### VARIABLE FRESH SNOW ALBEDO: HOW SNOWPACK AND SUB-NIVEAN PROPERTIES INFLUENCE FRESH SNOW REFLECTANCE

The understanding of albedo, or ratio of outgoing to incoming shortwave radiation, is necessary for modeling the melt characteristics of a snowpack in snow-dominated areas. The timing and supply of meltwater downstream is influenced by the energy balance, and albedo is used in those calculations. Current snow albedo models range from simple models that only reset albedo with new snowfall to complex models that are not feasible for most applications. We present a variable fresh snow model that enhances a simple albedo model, initially created by the U.S. Army Corps of Engineers, and used extensively in the Canadian LAnd Surface Scheme (CLASS). The new approach considers conditions prior to and during a snowfall event to improve fresh snow albedo estimates, instead of resetting to a static value; it also considers differences in the albedo decay rate.

Hourly shortwave radiation (incoming and outgoing), snow depth, temperature, and other meteorological data from two stations at the Senator Beck Basin in the San Juan Mountains of Southwest, Colorado were used for the period from 2005 to 2014. We evaluated changes in albedo of a high-elevation seasonal snowpack during fresh snow events and apply a set of multivariate regressions to recreate values of broadband albedo. The variable fresh snow albedo model approaches the Visible and Near-Shortwave Infrared portion of the electromagnetic spectrum differently and groups values by temperature. The model needs few inputs, specifically measurements of depth and temperature, an estimation of ground albedo, and for increased

accuracy, a quantification of the number of aeolian dust deposition events on the snowpack every year. This variable fresh snow model showed higher accuracy in albedo values, both of fresh and decayed snow ( $R^2$  of 0.77 and Nash Sutcliffe Efficiency, NSE of 0.75) than of CLASS ( $R^2$  of 0.67 and NSE of 0.62). When isolating fresh snow events, the variable fresh snow albedo model was much more accurate than the single-reset albedo provided by CLASS but still had a weak correlation to measured values ( $R^2$  of 0.38). The variable fresh snow albedo model especially outperformed CLASS during the melt period, with ~24% more accurate absorption values to measured values than CLASS. Since fresh snow albedo is primarily weighted by albedo from the timestep before, we suggest this model also be used to correct erroneous values of albedo given incorrect sensor measurements, such as due to snow accumulation on the upward looking shortwave radiation sensor (pyranometer).

## ACKNOWLEDGEMENTS

I want to acknowledge Jeff Derry, the director of the Center for Snow and Avalanche Studies for his stewardship and wisdom of the Senator Beck Basin Study Area and associated study plots. This work would not have been made possible without his commitment to ensuring the instrument towers are well-maintained and his accessibility to meet and share his extensive knowledge of the surrounding area. CSAS is lucky to have Jeff and I am grateful to have met him and his wife, Kim, through my studies.

I want to thank my advisor, Steven Fassnacht, for cultivating a space of curiosity and adventure for our lab during times of a global pandemic. Thank you for believing in me and providing suggestions when I faced roadblocks in my research and confusion in my results.

This work would have also not have been made possible without the generosity and support from my grandfather, Gunars. I will forever be grateful for your encouragement and backing of higher education, I am excited to do the same for my kids and grandkids. In many ways, this graduate degree further opened the door for me to do the same for others.

Lastly, I want to celebrate and call-out my family, friends, and lab group for their incredible support through it all. Especially during times of COVID-19, these people were at my side (mostly virtually) through the joys, difficulties, tears, and resolutions of it all.

Please enjoy.

## TABLE OF CONTENTS

ABSTRACT .....	ii
ACKNOWLEDGEMENTS .....	iv
CHAPTER 1. INTRODUCTION .....	1
1.1. Background .....	1
1.2. Previous Work.....	5
1.3. Research Motivation .....	9
CHAPTER 2. VARIABLE FRESH SNOW ALBEDO .....	11
2.1. Introduction .....	11
2.1.1. Background .....	11
2.1.2. Research Objectives .....	12
2.2. Study Site and Sensor Data .....	13
2.2.1. Senator Beck Basin Study Area .....	13
2.2.2. Red Mountain Pass Snow Telemetry Station.....	15
2.3. Methods.....	17
2.3.1. Dataset Preparation.....	17
2.3.2. Albedo – Niveometerological Correlation .....	23
2.3.3. Fresh Snow and Decay Albedo Model Creation .....	24
2.4. Results .....	26
2.4.1. General Snowpack and Albedo Characteristics (Snow Years 2006-2014).....	26
2.4.2. Data Evaluation .....	29
2.4.3. Estimating Broadband Albedo by Combining Wavelength Groups.....	32
2.4.4. Modeled Fresh Snow Albedo by Multivariate Regression .....	33
2.4.5. Assessing the Variable Fresh Snow Model .....	37
2.5. Discussion .....	42
2.5.1. Quantifying Fresh Snow Albedo .....	42
2.5.2. Late Season Influence on Albedo .....	45
2.5.3. Limits and Uncertainties in the Variable Fresh Snow Albedo Model.....	47
2.5.4. Suggested Improvements for Estimating Fresh Snow Albedo.....	49
2.6. Conclusion.....	51
CHAPTER 3. IMPLICATIONS .....	53
REFERENCES.....	55
APPENDIX A. ADDITIONAL EQUATIONS AND FIGURES .....	61
APPENDIX B. INDIVIDUAL SNOW YEAR RESULTS.....	63
APPENDIX C. MULTIVARIATE REGRESSION.....	68

## CHAPTER 1. INTRODUCTION

### 1.1. Background

The energy balance and melt of snow-driven watersheds dominate regional hydrology and climate in mountain regions around the world and areas where snow is seasonal in the winter. Snow- and/or glacial-melt is the primary source of water for one-sixth of Earth's population (Barnett et al. 2005). Due to the complexities and dynamics within the system, theorized correlations between variables, and the lack of quality data for each variable, modeling the energy required to melt snow requires multiple assumptions. The energy required to melt mountain snow (except in closed-canopy forest environments) usually comes from net shortwave radiation (Qu and Hall 2007), which is dependent on the optical properties of the snowpack as well as diurnal and seasonal changes in irradiance. During springtime, days lengthen providing more incoming solar energy to the system that can create a positive net energy balance to hasten melt. Snow is highly reflective, hence clean snow appears white and can remain even on sunny days.

Solar radiation primarily arrives to the surface as shortwave radiation (~100 nm to 5000 nm) and more than ~95% of this solar radiation arrives from wavelengths ~250 nm to 2500 nm. Shortwave radiation includes Ultra-Violet (UV), Visible (VIS), Near-Infrared (NIR), and Shortwave-Infrared (SWIR) portions of the electromagnetic spectrum; this radiation can be reflected, absorbed, or transmitted through some medium. Snow reflects each of these wavelengths differently, reflecting most in the visible spectrum and decreases as the wavelengths increase into NIR and SWIR (Warren 1982), though the size of the particle is also relevant and explained further below. In contrast, long wavelengths (>5000nm) are absorbed and re-emitted

by the particle and not influenced by the same properties of a snowpack as they are not reflected; this is known as longwave radiation, and not within the scope of this study. Other parts of the snow's energy balance are also relevant (**Figure 1-1**), but not as influential as net shortwave radiation on snowmelt in open, mountain regions, where this study will take place.

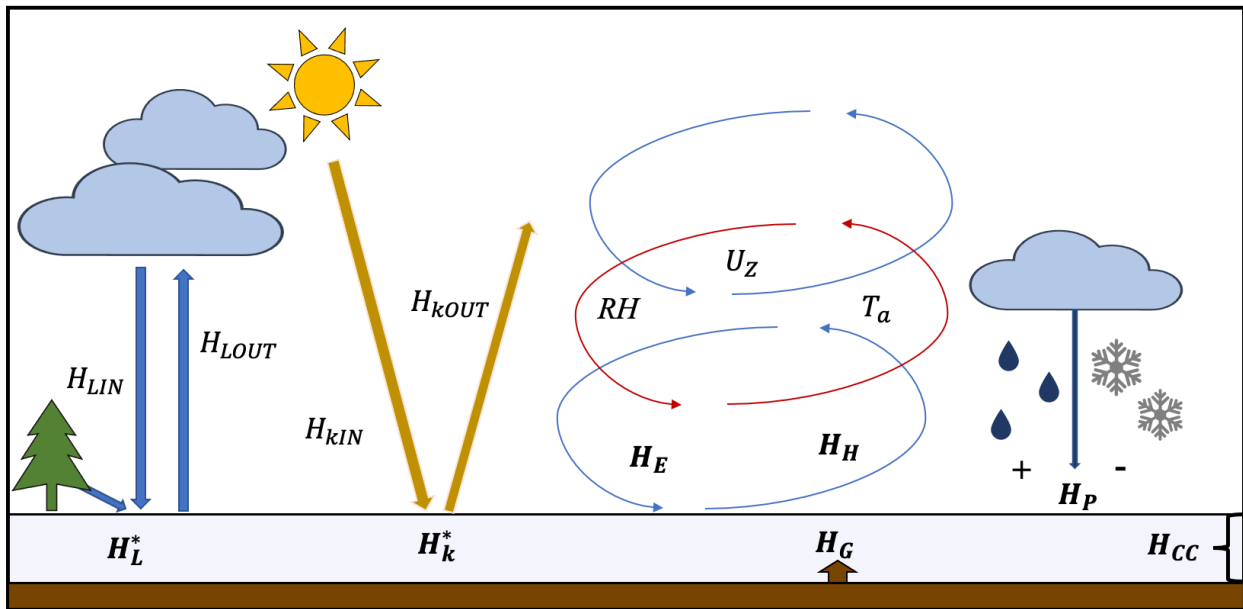


**Figure 1-1.** Conceptual diagram showing the energy budget of a seasonal snowpack, which is a measure of net longwave radiation ( $H_L^*$ ), net shortwave radiation ( $H_k^*$ ), measures of latent ( $H_E$ ) and sensible ( $H_H$ ) heat fluxes, energy from precipitation ( $H_P$ ), heat from the ground ( $H_G$ ), and the energy needed to overcome to induce melt ( $H_{CC}$ ). Other variables include relative humidity ( $RH$ ), wind speed ( $U_z$ ), and air temperature ( $T_a$ ).

Net shortwave radiation is either calculated as the difference of incoming minus outgoing shortwave radiation or by multiplying the incoming shortwave radiation by the albedo, which is the reflection coefficient of the surface. Snow reflects wavelengths differently and the term broadband albedo is used to describe the net reflection of shortwave radiation, independent of wavelength. Snow broadband albedo is the ratio of all outgoing shortwave to incoming shortwave radiation and is a function of the properties of the snowpack and changes with different snow characteristics and wavelengths, as well as the presence of any light absorbing particles (LAPs) (Dunkle and Bevans 1956; Warren 1982; Skiles and Painter 2018). Snow is a

porous medium, and shortwave radiation will penetrate the snowpack and be reflected, transmitted, or absorbed at layers below the surface. Depending on the trajectory of the photon, this radiation often goes through multiple-scattering events before re-emerging at the surface. This presents the idea that the characteristics below the surface play a role in albedo and need to be considered (**Figure 1-2**). For example, the albedo is less for a shallower snowpack as more shortwave radiation is absorbed by the ground surface below the fresh snow (left side of **Figure 1-2**) than for a deeper snowpack where the shortwave radiation has a higher likelihood of scattering internally and exiting the snow without encountering the ground surface.

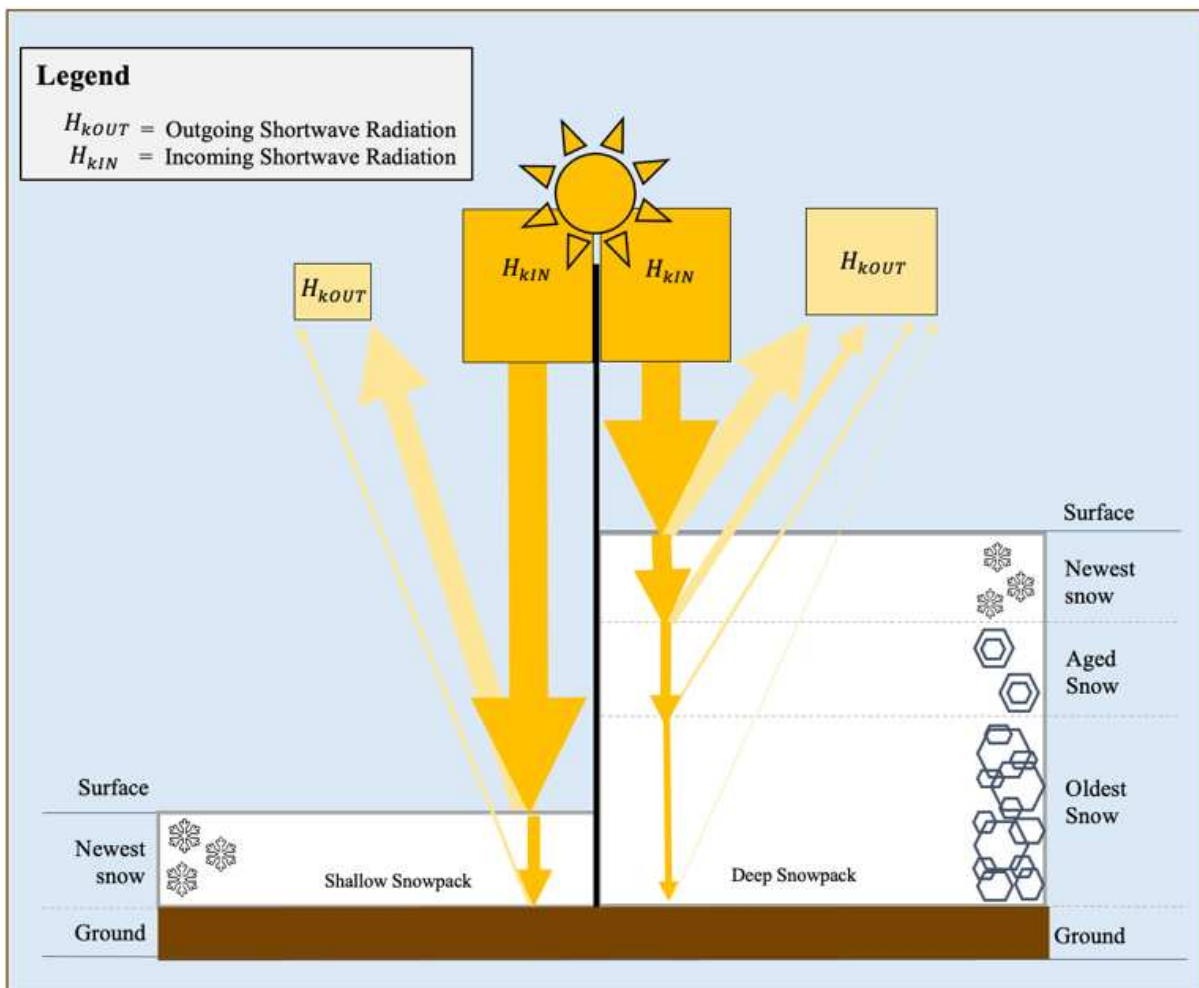


**Figure 1-2.** Conceptual diagram showing net solar radiation differences between a deep and shallow snowpack. The weights of the arrows indicate intensity of radiation.

Assuming the Beer-Lambert Law, light attenuates in a snowpack at a rate of  $e^{-kz}$ , where  $k$  is the extinction coefficient and  $z$  is the depth (Thomas 1962). The extinction coefficient is dependent on the snowpack's internal properties, grain shape and size, snow depth and density, as well as concentrations of any LAPs (i.e., black carbon, dust, ash, needles) (Bergen 1970; Reay et al. 2012; Burakowski et al. 2013). Papers dating back to the mid 20<sup>th</sup> century present the extinction coefficient range from  $0.1 \text{ cm}^{-1}$  (Thomas 1962) to  $1.5 \text{ cm}^{-1}$  (Mellor 1977), with the most common  $k$  values about  $0.2 \text{ cm}^{-1}$  (Liljequist 1956; Grenfall and Maykut 1977; Warren 1982). For example, if  $1000 \text{ w/m}^2$  of shortwave radiation entered a thirty centimeter snowpack and decreased in intensity at a rate of  $e^{-0.02/\text{cm}}$ , then only 1% of the radiation ( $10 \text{ w/m}^2$ ) would exist 22 cm below the surface, and more than half ( $>500 \text{ w/m}^2$ ) of the radiation would be extinguished within 4 cm from the snow's surface.

At the microstructure, snow grains undergo coarsening, grain growth, and sintering (grain bonding) that affects the shape, size, and count of individual grains (Colbeck 1980). Furthermore, changes in air temperature, precipitation, and relative humidity create gradients through the snowpack, that induces additional metamorphism through the snow that increases bulk density over time. Through microstructure kinetics and macrostructure gradients, snow grains are ever-changing as are the bulk properties of the snowpack, such as albedo; which are more widely used than internal snowpack properties in hydrologic models, meteorological models, climate models, or land surface schemes (Verseghy 1991; Vionnet et al. 2012).

Light extinction through a snowpack and broadband albedo are the basic shortwave radiative properties of snow, yet not often juxtaposed. They are related in that they both quantify the amount of solar radiation at a given point in snowpack, for albedo there is quantification of light exiting the surface, whereas light extinction quantifies the amount of shortwave radiation at

some depth in the snowpack. Conceptually, albedo can be considered a directionally upward measure of shortwave radiation and light extinction as directionally downward. However, this simplification undermines the complexities of light scattering through a medium comprised of vastly unique individual grains with differing reflectance properties. Yet, generally speaking, light extinction and albedo are of opposite direction and we consider the idea they may be related, at least that the properties which affect light extinction affect albedo.

## 1.2. Previous Work

The early work looking at light penetration into and off a snowpack involved mathematically solving for reflectance, which is a function of the scattering and absorption properties of a snow medium (Dunkle and Bevens 1956; Thomas 1962). It was found that a smaller snow particle reflects more light than its larger counterpart, and reflectance of a particle is dependent on wavelength, as visible light reflects more than near infrared for all particle sizes. This was confirmed both mathematically (Bergan 1970; Warren 1982) and experimentally (Nakamura 2001; Melloh 2002). These early authors often used simplified Mie scattering calculations to trace photon paths through the snow, and to use these calculations, one must assume the medium is comprised of non-sticky spheres. Snow grains are neither spherical nor non-sticky as they are adhesive. This led to another wave of research that used computer simulations to trace photon paths through semi-infinite mediums comprised of shapes and densities that better represent snow (Picard et al. 2009; Libois et al. 2013). These papers state that modeling light-snow interactions using a sphere-composed medium is inappropriate and underestimates the true reflectance. This improved our understanding of the reflectance properties of more realistic snow and researchers have improved these spherical models by incorporating parameters such as

specific-surface-area (SSA) and dendricity, which is a measure of crystalline structure of fresh snow before it rounds (Vionnet et al. 2012; Flanner and Zender 2006).

Researchers have proposed broadband albedo formulations that require different inputs and apply to varying snow environments (i.e., shallow versus deep snow, forested versus non-forested). A simple model albedo mode assumes that albedo decays with ageing snow at some rate and albedo is reset with fresh snow (US Army Corps of Engineers 1956; implemented by Verseghy 1991; Gray and Landine 1987; Gleason and Nolin 2016). Others have based albedo on the optical grain size near the surface and the age of snow, and calculated albedo separately for different wavelengths (Brun et al. 1992; Melloh et al. 2002; Vionnet et al. 2012). Albedo and albedo decay parametrization varies between snow models, from simple reset values to estimations of SSA and Mie Scattering reflectance.

SnowModel (Liston and Elder 2006) classify differences between albedo during times of melt and non-melt, however these are static values with a maximum albedo of 0.8. Albedo in SnowModel exists within the *EnBal* section of the model, where surface energy exchanges are considered. Variations in snow albedo due to LAPs or dense spring snow are not directly incorporated, but the model defines albedo separately for snow below forest canopies, snow in forest-free areas, and for glacier-ice (Liston and Elder 2006). Marks and Dozier (1992) separate albedo into visible ( $0.3 - 0.7 \mu m$ ) and near infrared shortwave infrared ( $0.7 - 2.8 \mu m$ ) portions of the electromagnetic spectrum in their alpine based energy balance model, which provides methods to iSnobal (Marks et al. 1999). Broadband albedo is not considered, but instead net shortwave radiation is found combining the two spectrally integrated albedos. Respective albedos are found by a function relating albedo decay inversely to the square root of the snow grain radii, where visible albedo decay is linear and near/shortwave infrared albedo decreases by

a first order decay. When reasonable grain radii are used and with a solar zenith angle of  $0^\circ$  visible albedo ranges from about 0.98 to 0.90 while near/shortwave infrared albedo ranges from 0.7 to 0.4. One less the cosine of the zenith angle accounts for changes in albedo with changing sun angles.

The Crocus model (Vionnet et al. 2012) also separates albedo into three spectral bands (0.3 – 0.8  $\mu m$ , 0.8 – 1.5  $\mu m$ , and 1.5 – 2.8  $\mu m$ .) The model also separates incoming shortwave radiation into the same three bands and uses empirical coefficients to divide the broadband radiation into each spectral band. Snow albedo in each band is a function of the optical diameters of the snow grains within the top three centimeters of the snowpack and the age of the snow. The impact of deposited LAPs on the snowpack is parameterized by the age of the snow in the visible spectrum (Vionnet et al. 2012). The optical diameter of the snow grain is found separately for dendritic and non-dendritic cases.

The SNow, Ice, and Aerosol Radiation model (SNICAR) is a multi-layer, two-stream radiative transfer solution (Flanner and Zender 2005; Flanner and Zender 2006). Snow is treated as a collection of ice spheres that are lognormally distributed in size with bounds set for a minimum (50  $\mu m$ ) and maximum (1000  $\mu m$ ) effective radius size. Mie scattering is the driver of SNICAR with Mie parameters (single scattering albedo, extinction coefficients, and asymmetry parameter) computed for one visible and four near/shortwave -infrared spectral bands. The model depends on vertically resolved effective radius, solar zenith angle, snow depth and density, direct and diffuse incident radiation, bare surface reflectance, and concentrations of absorbing impurities. Each variable mentioned has its own evolution through time and temperature gradients that are needed to compute bulk radiative transfer.

Due to its few inputs and justification for exponential decay, a commonly used albedo model is a simple first-order decay model suggested by the USACE (1956), which was implemented by Verseghy (1991) to solve for the albedo of snow in the Canadian Land Surface Scheme (CLASS):

$$\alpha_{s(t)} = [\alpha_{s(t-1)} - \alpha_{s-min}] * e^{-k\Delta t} + \alpha_{s-min} \quad [1-1],$$

where  $\alpha_{s(t)}$  is the albedo of snow for the current time step  $t$  which is computed from the albedo of the previous time step  $\alpha_{s(t-1)}$ ,  $k$  is the decay coefficient of the snow albedo,  $\Delta t$  is the length of the time step and  $\alpha_{s-min}$  is the minimum decay albedo depending on the ambient condition. The albedo is reset with new snow events and then subsequently decays at every time step thereafter. In CLASS, the albedo was reset to 0.84 with any amount of fresh snow while the decay coefficient is set to 0.01 per hour (Verseghy 1991). The only dynamic value is  $\alpha_{s-min}$ ; the snow can either be melting or have no-melt where the minimum value for decay is set to 0.5 or 0.7, respectively.

Gleason and Nolin (2006) calculated new coefficients for this general-decay model based on three years of post-fire albedo observations, adapting the equation to better represent effects from the LAPs that entered the system. The albedo decay coefficients ranged from 0.01 to 0.038 per hour with a melting, burned forest having the strongest decay with an earlier snow all gone (SAG) date, even if there was comparably larger SWE than in the controlled unburned site. Malik et al. (2014) also observed the decay during snowmelt to be quicker than the rest of the accumulation season once the snow became optically thin (< 0.5 m) and the “background” albedo began to influence albedo. Treating the snowmelt melt period uniquely from the rest of the season increased the accuracy of melt-rate, stream runoff, and evapotranspiration estimations

at the basin scale (Malik et al. 2014). In addition to better representing subsurface grains on broadband albedo during melt process, treating the snowmelt period separately also allows LAPs to be more easily incorporated within models (Bryant et al. 2013). As the snow melts, dust and other LAPs compound and resurface (Skiles and Painter 2018), unlike dissolved constituents (ions etc.) that are captured by meltwater and flushed from the system (Bales et al. 1989).

The effect of LAPs on snow albedo is an active research field that illustrates the decreased albedo due to LAPs including aeolian-deposited particles such as dust, black carbon, aerosols, and soot, which increases radiative forcing on snow, increases melt, and affects runoff timings for snow-driven watersheds (Painter et al. 2012; Skiles et al. 2012; Reay et al. 2012; Libois et al. 2013). More specifically in the Colorado Rocky Mountains, where this study takes place, aeolian-deposited dust onto and then within the snowpack affects basin-scale melt (Skiles et al. 2012; Painter et al. 2012); the primary source of this dust comes from the southern Colorado Plateau (Skiles et al. 2015). Neff et al. (2008) has suggested evidence that the larger and more frequent dust events are a relatively new phenomena, since disturbance and settlement of the West in the 1870s. Furthermore, these dust events are expected to intensify with a warming climate due to sustained drought and increasing temperatures that reduce vegetation cover. This reduction in vegetation increases disturbance to the biological soil crust and increases wind erosion that further increases the sediment available for aeolian dust emissions (Munson et al. 2011).

### 1.3. Research Motivation

In the snow- and glacier- hydrology community, the albedo of snow and ice has been highly scrutinized with multiple formulations of how to estimate broadband albedo. Optimally, a model could adapt to changing conditions, yet require a minimum of input parameters, such as

meteorological and snowpack data. Though the CLASS formulation (equation 1-1) shows promising results for its simplicity as users can adjust the albedo decay coefficient, no prior research has evaluated the reset values of the formulation of fresh snow. Since it is a first order decay function, this reset value drives that decay that follows, and erroneous fresh snow albedo values will inevitably lead to erroneous albedo values.

Increases in aeolian dust via human settlement (Neff et al. 2008) and changes in climate (Rasmussen et al. 2011) provide a real threat to accurate estimations of snow melt rates and the timing of SAG dates. Additionally, increases in fires across the Rocky Mountains (Schoennagel et al. 2004) also provide LAPs and lower ground albedo values via burnt soil that both can expedite melt. It is imperative to capture these variables in net shortwave radiation computation, especially during the late season, as to not underestimate radiation of a seasonal snowpack that provides water resources for all downstream.

## CHAPTER 2. VARIABLE FRESH SNOW ALBEDO

### 2.1. Introduction

#### 2.1.1. Background

Both light extinction and the broadband albedo of a snowpack have been studied extensively from a physical (Bergan 1970; Warren 1982; Flanner and Zender 2006) and experimental perspective (Nakamura 2001; Melloh 2002; Burakowski et al. 2013) and have been found to be highly variable. A first order albedo decay model, though simple in its requirements (USACE 1956; Verseghy 1991), does not account for the dynamics within a snowpack that create the variation in albedo values. Recently researchers have been modeling albedo with a more physical approach describing microstructure kinetics (Flanner and Zender 2006; Vionnet et al. 2012), which is similar to the physical and mathematical approach previously used to calculate snow albedo (Dunkle and Bevans 1956; Bergan 1970; Bohren and Barkstrom 1974; Warren 1982).

Easy-to-use models often use a pre-determined value that ‘resets’ fresh snow albedo to a maximum when there is enough new snowfall. Fresh snow albedo reset values range from 0.80 to 0.85 (Verseghy 1991; Malik et al. 2014; Gleason and Nolin 2016) with some models requiring there to be a minimum amount of new snowfall ( $\sim 0.03$  m) for albedo to be completely reset (Brandt et al. 2005). Current and simple albedo models tend to overestimate albedo during spring melt, which incorrectly underestimates melt rates and lengthens the snow cover duration, mainly due to incorrect decay rates that do not include background effects (Malik et al. 2014) nor the effects from light absorbing particles (LAPs) (Gleason and Nolin 2016; Painter et al. 2012; Skiles et al. 2012). Models such as iSnobal (Marks et al. 1999), SNICAR (Flanner and Zender

2006), and Crocus (Vionnet et al. 2012) are physically based and show promising albedo results, especially when considering changes in irradiance, snow metamorphism, and additions of LAPs. However, these models often need variables that must be assumed or estimated, which can decrease the accuracy of the model when uncertain or incorrect assumptions are made. In areas with limited knowledge, incorrect assumptions will inevitably lead to shortened or lengthened snowpacks, with a larger magnitude corresponding to the bias of the assumption.

We seek a model that needs few inputs and uses few assumptions, which can estimate albedo and albedo decay simply and effectively, yet also incorporates more physically based variables that describe surface and underlying properties of the snowpack. We propose that these subsurface properties affect the broadband albedo when fresh snow falls, with the intent of this study to provide more representative albedo reset values. The goal is to enhance a simple albedo decay model to better quantify shortwave radiation absorption of a seasonal snowpack so that the dynamics of fresh snow albedo and the subsurface layers are better represented with limited inputs. This new formulation will be tested against the current formulation to illustrate the improvement in modeled net shortwave radiation to measured values.

### *2.1.2. Research Objectives*

Using meteorological and snowpack data, our objectives are to:

1. Assess, define, and adjust a meteorological and snowpack (niveometeorological) dataset for use in creation of a new fresh snow albedo formulation. This will consider a) corrections to incoming and outgoing shortwave radiation measurements, b) an evaluation of the daily time series to zenith angles, c) evaluation of snow depth changes during snowfall accumulations, and d) assess differences in albedo change across the shortwave radiation spectrum;

2. Determine the correlation between nivo-meteorological variables and albedo; and
3. Create a new albedo model formulation to incorporate nivo-meteorological variables and spectrum considerations into estimating fresh snow albedo and decay.

Addressing these objectives will improve our understanding of the importance that subsurface snow grain and ground characteristics have in broadband albedo models. It will also suggest ways to improve the accuracy of albedo modeling by improving fresh snow values, especially where radiation data might be lacking.

## 2.2. Study Site and Sensor Data

### 2.2.1. Senator Beck Basin Study Area

The Senator Beck Basin Study Area (SBBSA) is operated by the Center for Snow and Avalanche Studies (CSAS) near Red Mountain Pass, located in the San Juan Mountains of Colorado of the Southern Rocky Mountains. Serving as a high-elevation research watershed, SBBSA (2.91 km<sup>2</sup>) lies at the headwaters to the Uncompahgre River in the Upper Colorado River Basin and has an elevation ranging from 3362 to 4118 meters. The adjacent area is a mix of primarily herbaceous, barren land, and evergreen forests. Since 2003, hourly, meteorological and snowpack data have been automatically collected at two study plots. We used these data for nine consecutive seasons during the Snow Year (SY) of 2005 to SY2014, as these years have been analyzed before and the corrected radiation data to more realistic values have been made accessible (Painter et al. 2015; Skiles et al. 2015). The SY runs from September 1<sup>st</sup> to August 31<sup>st</sup> of any given two years and is used instead of Water Year, since snow events occur before October 1<sup>st</sup> at SBBSA and this work tracks patterns of snowpack albedo.

### *Swamp Angel Study Plot*

The sub-alpine Swamp Angel Study Plot (**Figure 2-1**) (SASP; 37.9069°N, 107.7113°W) is at an elevation of 3371 meters and sits within a grassy forest clearing surrounded by Evergreen trees. This setting acts to lessen the influence of wind, which makes it optimal for snowpack and precipitation measurements (Landry et al. 2014). Throughout the year, wind stays consistent and has no seasonal influence. Wind averages 0.9 m/s and with a maximum approaching 5.5 m/s. We used hourly incoming shortwave radiation ( $H_{kIN}$ ), air temperature ( $T_a$ ), wind speed ( $U_z$ ), outgoing shortwave radiation ( $H_{kOUT}$ ), and snow depth ( $d_s$ ) data (**Table 2-1**) from SASP that are archived by CSAS <<https://snowstudies.org/archived-data/>>. Dust events ( $DE$ ) were recorded daily as they happened, and this information has been published since 2006.

#### *Senator Beck Study Plot*

The alpine Senator Beck Study Plot (SBSP; 37.9069°N, -107.7263°W) is at an elevation of 3714 meters and is located above treeline. SBSP is strongly influenced by wind as it is in an exposed alpine tundra landscape. Winds average 3.5 m/s throughout the year; the windiest months occur in Wintertime from December to April, with hourly averages wind speeds reaching upwards of 16 m/s. We used the same automated sensor data (**Table 2-1**) as per SASP, retrieved from the CSAS online archives.

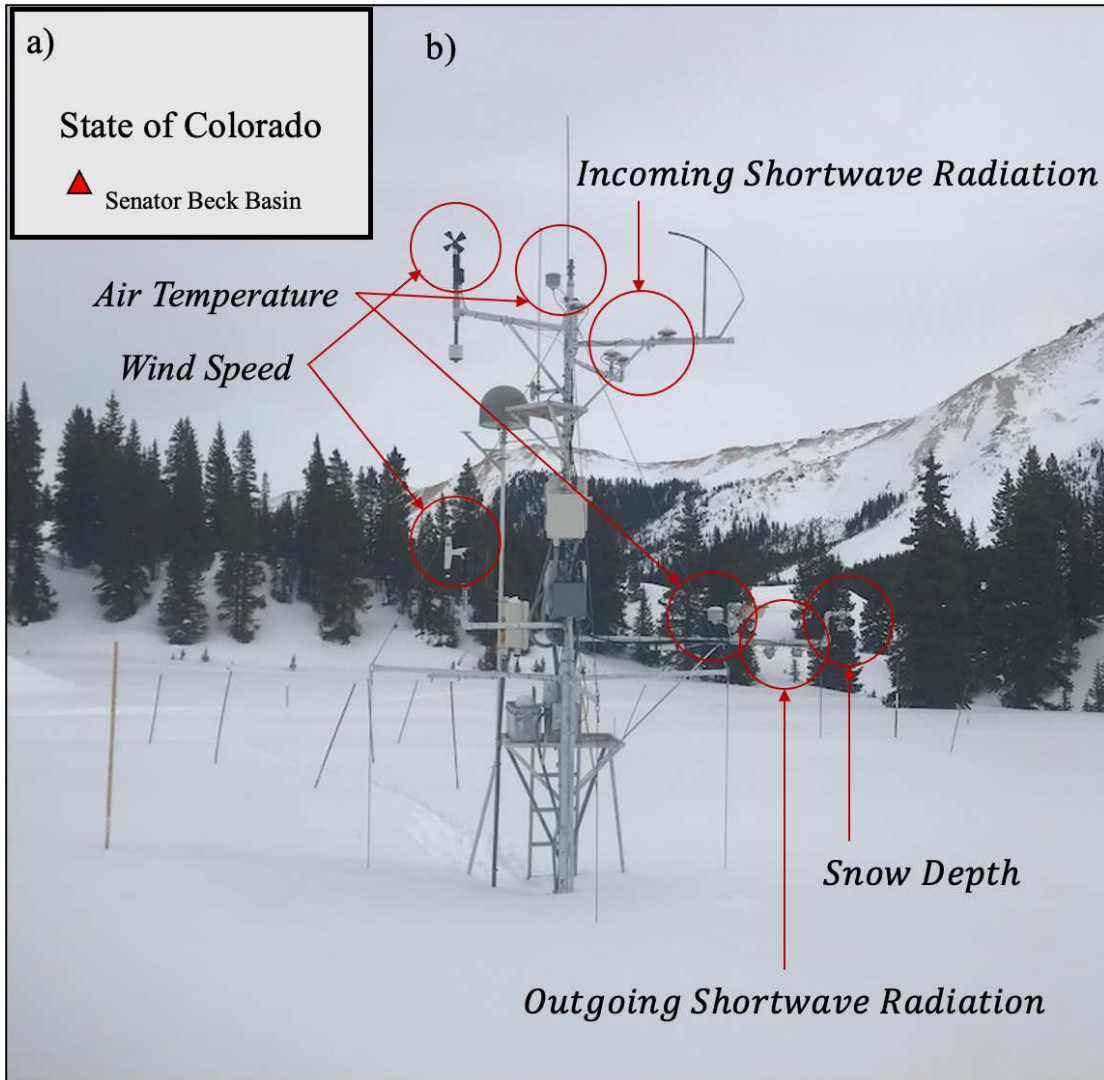


**Figure 2-1.** Instrumentation tower at Swamp Angel Study Plot within Senator Beck Basin in Southwest Colorado (a). The tower at SASP (b) stands 6 meters tall whereas the tower at SBSP (not-pictured) stands 9.6 meters tall.

### 2.2.2. Red Mountain Pass Snow Telemetry Station

The Red Mountain Pass Snow Telemetry (SNOTEL) station, operated by USDA Natural Resources Conservation Service (NRCS), sits at approximately 37.9°N, 107.7°W and 3414 meters in elevation. The SNOTEL station is several kilometers away from SASP on the east side of Highway 550, just south of Red Mountain Pass. The Red Mountain Pass station is the spatially closest SNOTEL to SBBSA and has measurements of snow depth and SWE per day.

Data from SNOTEL were downloaded using the [RNRCS package in R](#), but can also be found using the NRCS Red Mountain Pass SNOTEL website: <https://www.wcc.nrcs.usda.gov/>.

**Table 2-1.** Automated Sensor Data for SBSP, SASP, and SNOTEL, including Variable Measured, Parameter Label, Active Sensor, and its Sensitivity

Variable	Label	Site	Active Sensor	Sensitivity
Incoming Solar Radiation	$H_{kINbrbd}$	SASP & SBSP	<a href="#">K&amp;Z CM21 Pyranometer</a>	Broadband: 305-2800 nm
	$H_{kINNSWIR}$		<a href="#">K&amp;Z CM21 RG695 Pyranometer</a>	Near & Shortwave IR: 780-2800 nm
Reflected Solar Radiation	$H_{kOUTbrbd}$	SASP & SBSP	<a href="#">K&amp;Z CM21 Pyranometer</a>	Broadband: 305-2800 nm
	$H_{kOUTNSWIR}$		<a href="#">K&amp;Z CM21 RG695 Pyranometer</a>	Near & Shortwave IR: 780-2800 nm
Air Temperature	$T_a$	SASP	<a href="#">Vaisala CS500, HMP50YA</a>	Measured to 0.1°C, increased error with warmer & colder temperatures
		SBSP	<a href="#">Vaisala HMP50YA</a>	
Snow Depth	$d_s$	SASP & SBSP	<a href="#">CSI SR50 Ultrasonic Distance Ranger</a>	Measured to 0.001 meters, accuracy to 0.01 meters
Wind Speed	$U_z$	SASP & SBSP	<a href="#">RM Young Wind Monitor 05103-5</a>	± 0.3 meters per second
Snow Water Equivalent	SWE	SNOTEL	Snow pillow using <a href="#">100" Transducer - Sensotec</a>	± 0.1 inch; ± 2.54 millimeters
Snow Depth	$d_s$	SNOTEL	<a href="#">Temperature corrected ultrasonic depth sensor</a>	± 1 inch; ± 0.0254 meters

## 2.3. Methods

### 2.3.1. Dataset Preparation

The SASP and SBSP hourly datasets required some manipulation prior to estimating the correlation between the meteorological and snowpack (niveometeorological) data and albedo. The data preparation includes evaluation of the shortwave radiation measurements, consideration of the zenith angles with respect to albedo, implications of the magnitude on snow depth increases during snowfall accumulation, and consideration for differences in albedo change across the shortwave radiation spectrum.

#### 2.3.1a Incoming and Outgoing Solar Radiation Adjustments

We used data from two upward facing and two downward facing pyranometers that measures shortwave radiation at each Study Plot in Senator Beck Basin (**Table 2-1**). Low shortwave values measured from the upward pyranometer due to snow accumulation on the sensor can yield albedo values greater than 1. Due to errors with measurements from the downward facing pyranometer caused from a non-level reflection surface, computed albedo may be less than 0. Therefore, the incoming and outgoing radiation values were considered separately to correct erroneous albedo calculations. Errors were due to snow accumulation on the sensor, a non-level reflection surface, and albedo difference for different wavelengths. Outliers of incoming and outgoing radiation were identified by albedo values of greater than one or less than zero. SASP receives low wind as it is protected by the surrounding forest and new snow often accumulates on the sensor. Conversely, SBSP sits in the alpine and continuous wind gusts blow off any snow accumulating on the equipment. Replacing albedo values at SASP from SBSP instead of incoming shortwave radiation values at SASP from SBSP showed a better correlation ( $R^2$  of 0.5 versus  $R^2$  of 0.33) when comparing estimated SASP albedo to observed SASP albedo

(Figure A-1). Therefore, during times at SASP when the albedo was greater than one, we used the albedo from SBSP for the same hour and then solved for the incoming radiation:

$$H_{kIN_{SASP}} = \frac{H_{kOUT_{SASP}}}{\alpha_{SBSP}} \quad [2-1]$$

Outgoing shortwave radiation measurement is necessary to calculate albedo, and yet it is not common at meteorological stations. The surface below a downward facing pyranometer needs to be open and planar so the measurement is not affected by directly-adjacent surfaces; the surface also needs to be flat so that the direction of the reflected photon has little influence from topographical changes in the surface also considering the scattering-angle of the photons as the position of the sun changes through the day. SASP exists within an open-field and SBSP is above treeline, so neither site is influenced by tree cover. Given that both pyranometers are estimated to be level within 1° post-installation (Landry et al. 2014), the upward facing pyranometer measures the hemispherical radiance on a level surface, and the downward facing pyranometer measures the reflected radiance on a snow's surface where the gradient of the surface is dependent on the properties below. The characteristics of the snow surface are highly variable as snow falls unevenly, wind redistributes sporadically, and snow melts heterogeneously (Fassnacht et al. 2009), inevitably creating an uneven surface where readings of outgoing shortwave radiation and therefore a direct albedo ratio calculation will be erroneous (Jonsell et al. 2003). Painter et al. (2012) used a scalar that can be applied to incoming radiation to calculate the difference from the cosine of local zenith angle to the cosine of the solar zenith angle. The cosine of the local zenith angle was found by a function involving the solar zenith angle, slope, and aspect of the surface of the snow surface (see equations [A-1] and [A-2] in Appendix A).

Corrected radiation data can be found from Skiles (2019) that is published online <<http://doi.org/10.5281/zenodo.2532590>>.

### *2.3.1b Zenith Angle Considerations*

The zenith angle changes diurnally as the sun rises and sets daily, and seasonally as the Earth and its axial tilt orbits the sun changing the daily maximum angle of the sun in the sky, as well as increasing and decreasing the length of the day through the year. The time at which the sun is at its highest point in the sky is called solar noon, with the most direct (and largest clear-sky values of) incoming solar radiation for a day. Some researchers only use values from solar noon as these tend to be the most accurate readings of albedo with less influence from sun angle (Burakowski et al 2012; Malik et al, 2014), while others have corrected high albedo readings for low zenith angles and then used albedo readings for all daylight hours (Painter et al. 2012; Skiles et al. 2012). We are interested in not only accurate albedo values provided at solar noon, but also the change in albedo when there is new snowfall, with the measurement time step of one hour. Due to its location on Earth, the zenith angle at Senator Beck Basin fluctuates from 14° at the summer solstice to 61° at the winter solstice. Though solar noon values at SBBSA fluctuate from 1156 to 1226 MST, the sensors are automated to record on the hour, every hour, with the closest time to solar noon being 1200 every time.

Snow albedo typically increase around dawn and dusk (Fassnacht et al. 2001), due to the large zenith angle and extreme angles at which the shortwave radiation arrives to the snowpack (Melloh et al. 2002). Therefore, at SBBSA, we used hourly values at 1000, 1100, 1200, 1300, and 1400 to ensure enough incoming and thus outgoing shortwave radiation when quantifying fresh snow albedo. This is roughly +/- two hours to solar noon. Therefore, if there was new snowfall during this timeframe, there was a five-hour timeframe to assess how albedo changed,

without the influence from low zenith angles. For the nine SYs, this filter yielded 35,066 observed albedo values from the two study plots. Calculated hourly changes in depth, temperature, and albedo were computed to assess changes in meteorological and sub-nivean properties in juxtaposition to changes in albedo during these five hours.

### *2.3.1c Snow Depth Changes During Snowfall Events*

Snow depth is often automatically measured using the time it takes for an ultrasonic pulse to travel to a surface and back (Ryan et al. 2008). The SBBSA study plots both use a Campbell Scientific SR-50A Ultrasonic Distance Ranger that measures snow depth to the nearest millimeter. The stated accuracy of the SR-50A is one centimeter, or 0.4% the distance to the target, so we rounded all snow depth values to the nearest centimeter. Ryan et al. (2008) showed the sensitivity of these sensors to be about two centimeters, showing inaccuracies even at one centimeter due to surface roughness differences caused from wind scour and wind drift. More frequent snow depth measurements improve the accuracy of the change in snow depth due to snowfall, as longer intervals also increase the amount of metamorphism that has occurred on and below the surface (Fischer 2011).

The sensors at SBBSA that record hourly snow depth provides frequent measurements, although fresh snow events can be less than an hour long, and metamorphism starts immediately. This one-hour time step also means that incremental amounts of snow added would be smaller than observations every three hours or more. Thus, magnitude of snowpack increase in an hour is often the same or less than the accuracy of the snow depth measurement. A solution is to use the longer time step; however, the focus is to examine hourly fluctuations in albedo to improve the hourly decay model (e.g., equation 1-1). A longer time step may result in missing when fresh snow albedo is at its maximum; more metamorphism may occur between measurements leading

to albedo decay and decreasing values of albedo. The hourly time step would better capture the snowstorm layer by layer to calculate change of albedo with additional fresh snow on fresh snow; it also better captures fresh snow immediately falling on older snow. We chose to calculate changes in depth from one hour to the previous and flag changes that were equal to +0.01 meters, due to the uncertainty associated with the depth sensor.

### *2.3.1d Wavelength Considerations*

The shortwave radiation is measured at SBBSA as unfiltered (broadband) and filtered (near- and shortwave-infrared) radiation (**Table 2-1**). The unfiltered incoming radiation less the filtered incoming radiation is the radiation that arrives to the snowpack in the visible spectrum (equation 2-2). When there is cloud cover, more near-infrared (NIR) and shortwave-infrared (SWIR) radiation are absorbed by the clouds than visible radiation (Melloh et al. 2002).

Therefore, with clouds, less total incoming shortwave radiation arrives to the snowpack, but it arrives more as visible light, of which snow and ice reflect more than NIR and SWIR; this increases albedo with all other variables staying constant (Warren 1982). Though clouds affect incoming and outgoing solar radiation values, high broadband albedo readings during times of snow (>0.9) can exist and need to be considered as the snowpack receives very little energy from net shortwave radiation during this time and removing these values overestimates absorption.

Light absorbing particles lower the albedo of a snowpack during times of melt as the LAP layers start to re-emerge with decreased depth, and this helps to accelerate melt even further by increased radiative forcing of the radiation on the particles (Painter et al. 2012; Skiles et al. 2012; Gleason & Nolin 2016). LAPs are darker and absorb more shortwave radiation than snow does in the visible spectrum. At Senator Beck Basin, LAP layers primarily come from aeolian dust that is carried via wind from the Southwest (Painter et al. 2007; Neff et al. 2008). These dust

events have been recorded by CSAS since October of 2006 and events span multiple days at a time. During spring melt these dust layers re-emerge and more visible radiation is absorbed by the LAPs, thus reducing broadband albedo. The difference in reflection between the visible and NIR/SWIR portion of the spectrum on the same medium justifies the need to separate albedo by wavelength, as to capture light reflecting properties differently. Using the two types of pyranometers at each Study Plot we were able to calculate the reflected radiation in the visible spectrum:

$$\alpha_{vis} = \frac{H_{kOUT_{vis}}}{H_{kIN_{vis}}} = \frac{H_{kOUT_{brbd}} - H_{kOUT_{NSWIR}}}{H_{kIN_{brbd}} - H_{kIN_{NSWIR}}} \quad [2-2]$$

The number of dust events were summed every day for each snow-year so that by the final dust event, the number of events would be at a maximum and reset the next snow-year. Therefore, on any given day and hour this provides a count of dust layers that exist below the surface and will collectively re-emerge during melt. Physically these LAPs lower albedo in the visible portion of the spectrum, and this provided justification to split snow albedo into the visible ( $\alpha_{vis}$ ) and the NIR/SWIR ( $\alpha_{NSWIR}$ ) portions of the spectrum so they can be evaluated separately. SASP and SBSP both have broadband and NSWIR measurements (**Table 2-1**) and thus the ability to calculate the visible portion possible. We to apply a linear model so that:

$$\alpha_{brbd} \sim k_{vis}\alpha_{vis} + k_{NSWIR}\alpha_{NSWIR} + C \quad [2-3]$$

where  $k$  is a weighted coefficient and  $C$  is a constant that corrects for discrepancies.

All reasonable ( $\alpha_{brbd} < 0.98$ ) daytime data across the nine snow years were divided into a calibration period (SY2006 – SY2011) and an evaluation period (SY2012 – SY2014). Two sets of hourly data were considered: all measurements during the daytime, or “all-snow”, and data from “fresh-snow” events, which are described in the next section. For “all-snow”, 73% of

datapoints ( $n = 44657$ ) were used for calibration and 27% for evaluation. For the fresh-snow linear model, 70% of values ( $n = 862$ ) were used in the model calibration and applied to the remaining 30% for evaluation. To assess model accuracy, we calculated the correlation coefficient ( $R^2$ ) and Nash-Sutcliffe Efficiency Coefficient (NSE; Nash and Sutcliffe 1970).

### 2.3.2. Albedo – Niveometerological Correlation

New snow albedo values were identified for hours ( $t$ ) when there was an increase in both broadband albedo and snow depth. Albedo values slightly fluctuate over the day even if depth stays consistent (Melloh et al. 2002) and observing new snow by increases only in albedo would likely overestimate the amount of new snow events. Secondly, snow depth sometimes increased (potentially indicating new snow), but albedo concurrently decreased, which does not occur with the concept that fresh snow resets albedo. Such values were attributed to changes in zenith angle or uncertainty with the depth sensor. Therefore, fresh snow events were identified by both positive changes in hourly albedo and hourly depth.

After identifying the fresh snow time steps at both study plots, the correlation was computed between fresh snow albedo, meteorological and snowpack conditions. Changes in albedo were juxtaposed with changes in depth, depth of the underlying snow, temperature, temperature from the time step prior, albedo from the time step before, wind speeds, relative humidity, and calculations of vapor pressure. Using multiple fresh snow density ( $\rho_{s_{fresh}}$ ) models (Diamond and Lowry 1953; LaChapelle 1961; Hedstrom and Pomeroy 1998; particle shape model by Fassnacht and Soulis 2002) (Appendix A), and calculated bulk snowpack density ( $\rho_{s_{bulk}}$ ), computed from the Red Mountain Pass SNOTEL SWE and depth measurements, we compared fresh snow albedo with estimates of fresh and bulk snowpack densities. Furthermore, we explored the correlation between temperature and fresh snow albedo. Snow crystals at

warmer temperatures are more susceptible to melting and their crystalline structure is more vulnerable to decay by melting and refreezing processes, especially compared to snow crystals that exist at very cold temperatures. It is difficult to estimate the shape of snow crystals based on near-surface temperature and vapor pressure alone. Snow crystals form in the atmosphere and experience dynamic meteorological conditions as they fall between their formation and the ground (Libbrecht 2005), which makes the shapes as they land nearly impossible to predict. However, given the sensor data availability, we used air temperature during fresh snow events as an independent variable with broadband albedo as the dependent.

### *2.3.3. Fresh Snow and Decay Albedo Model Creation*

Using the fresh snow time step data, we created four multivariate regression models that are binned by two temperatures groups with a threshold of the three degrees Celsius and two wavelength intervals discussed earlier (Warm-VIS, Cold-VIS, Warm-NSWIR, Cold-NSWIR). Variables for the regression model were chosen based on results from the albedo and nivometerological correlations. The coefficients and variables of the models were found for each temperature bin and wavelength interval and then evaluated with the measured albedo of the same bin and wavelength group. Afterwards, the visible albedo and NIR/SWIR albedo values were combined into broadband albedo using weighted coefficients from equation 2-3 for both the “all-snow” and “fresh-snow” models. In this regression, fresh snow broadband albedo is calculated from the estimations of visible and NSWIR albedo that were separated by two temperature groups and used multiple nivometerological variables. The nivometerological variables include some combination of hourly snow depth ( $d_s$ ), hourly change in snow depth ( $\Delta d_s$ ), albedo from the time step before ( $\alpha_{(t-1)}$ ), number of dust events (DE), and air temperature ( $T_a$ ).

We have hourly measurements from the sensor data for all the variables but need to assume albedo from the previous time step to calculate fresh albedo. When the first snow accumulates on the bare ground, we can assume  $\alpha_{(t-1)}$  is the broadband albedo of the ground. We chose 0.2 as the ground albedo as this value was both calculated during times of no snow depth and validated by knowing the vegetation type below the instrumentation towers. Therefore, when there was new snow, albedo from the timestep before could be assumed and fresh snow albedo calculated. If zero snow depth was recorded, albedo was assumed to be 0.2 (ground albedo).

If there was no fresh snow at hour  $t$ , but snow depth was greater than zero meters, we used a first order albedo decay model (equation 1-1) from USACE (1956) and Verseghy (1991). Using results from Malik et al. (2015), Gleason and Nolin (2006), and Skiles et al. (2012), we chose to use two decay coefficients to accommodate accelerated melt during the late season due to increased incoming solar radiation, reemergence of LAPs, and larger surface and subsurface grains due to metamorphism and melt-refreeze processes that decrease reflectance. The magnitude of incoming shortwave radiation changes seasonally due to the cosine of the zenith angle and the amount of sunlight received daily. Large incoming shortwave radiation values occur in spring, even weeks before the summer solstice; this increases the melt decay rate which increases the albedo decay rate, by larger quantities of liquid water, snow grain size, and snow grain roundness. To account for this increase in melt during the late season we adjusted the albedo decay rate ( $k$ ) during warm temperatures ( $\geq 3^{\circ}\text{C}$ ) to a function of the cosine of the daily maximum zenith angle,  $\theta_{z_{dmax}}$ , weighted by some constant ( $c$ ) that sets bounds so that the average value of  $k$  is 0.01 per hour (equation 2-4). During times of non-melt and cold temperatures ( $< 3^{\circ}\text{C}$ ) snow albedo decays slower and is set to 0.005 per hour.

$$k = \cos(\theta_{z_{dmax}}) * c \quad [2-4]$$

Since the decay rate determines computed albedo, and the albedo at the previous time step (t-1) affects the albedo at the current time step (t), it was important to accurately model the decay rate which would help improve the accuracy of the fresh snow albedo computation, which subsequently increases the accuracy of the albedo decay computation. Incorrectly estimated albedo values at the beginning of the season have a chance to propagate through the start of the season. However, the middle of the snow season, with its colder temperatures and more frequent snowstorms stabilizes high albedo reset values. Even though the longevity of the error seems large at the start of snow season, albedo experiences slow decay and high fresh snow albedo reset values during accumulation that maximizes albedo, with bounds of less than 0.97, and prevents error-propagation.

## 2.4. Results

### 2.4.1. General Snowpack and Albedo Characteristics (Snow Years 2006-2014)

The two study plots at Senator Beck Basin are typical high elevation, deep seasonal snowpacks, with accumulation starting in late fall, with a peak depth occurring in spring that often surpasses 2 meters in depth (**Table 2-2** and **Figure 2-2**). Over the nine study years, SY2012 had the least snow at SBSP, with a maximum depth of 1.39 m, where SY2008 has the most snow at SASP and SY2006 had the most snow at SBSP (**Table 2-2**). Snow-All-Gone (SAG) dates happen prior to the summer solstice in most years, but SAG depends on the precipitation patterns prior to peak depth, peak SWE amount, and the quantities of precipitation and net shortwave radiation during melt. The SAG date at SBSP occurred either later than or on the same SAG date at SASP (**Table 2-2**; Duskocil et al. 2021), where due its lower elevation and

warmer temperatures, often melted out sooner. The deepest snow years provide the most amount of snow to the system, and for these nine of years of data SY2008 and SY2011 were just under 3 meters at peak depth, with about 850 mm of peak SWE, and were the ‘wettest’ years. In contrast, SY2012 and SY2013 were quite dry, being the only years with shallower than 2 meters in depth and less than 500 mm of SWE (**Table 2-2** and **Figure 2-2**).

**Table 2-2.** Peak depth and Snow-All-Gone dates at Swamp Angel and Senator Beck Study Plots, with Red Mountain Pass SNOTEL Snow Water Equivalent, and peak density and associated dates. Number of Dust Events was measured at SASP.

Snow Year (9/1 - 8/31)	SASP		SBSP		SNOTEL		# Of Dust Events
	Peak Depth (meters)	SAG	Peak Depth (meters)	SAG	Peak SWE (mm)	Peak Density (kg/m <sup>3</sup> )	
SY2006	2.62 7 April	27 May	2.31 7 April	9 June	602 5 April	380 17 May	7
SY2007	2.08 4 April	5 June	2.08 5 May	21 June	602 8 May	429 1 June	8
SY2008	2.91 11 April	16 June	1.88 11 April	18 June	861 17 April	428 6 May	7
SY2009	2.33 18 April	21 May	1.71 17 April	21 May	699 18 April	482 17 May	8
SY2010	2.43 26 March	29 May	1.94 24 April	9 June	599 9 April	419 8 May	9
SY2011	2.80 26 April	23 June	2.31 19 May	27 June	856 22 May	412 31 May	10
SY2012	1.97 28 February	11 May	1.39 19 March	21 May	452 20 March	499 11 May	8
SY2013	1.78 4 March	19 May	1.58 16 April	1 June	498 25 April	459 22 May	8
SY2014	2.26 7 April	7 June	1.58 7 April	12 June	622 1 May	499 8 June	10

During early season snow events, when snow falls and melts away before seasonal accumulation, albedo increases rapidly from ground levels. The early season albedo values are dependent on the frequency of snow events (**Figure 2-2**). Years with fewer snowfalls often have little to no underlying snow depth, which exposes the dark ground that both decreases fresh

snow albedo and speeds melt, this makes albedo highly variable until snowpack accumulation starts (**Figure 2-2**). Once snow persists on the ground, the range of the snowpack albedo variability narrows to about 0.74 to 0.9, which are albedo values that are commonly associated with snow. Albedo starts decreasing around peak depth, when snow grain rounding, and snowpack densification start to occur. Most often this time happens around DOSY 227 or April 15<sup>th</sup> +/- one month (**Table 2-2** and **Figure 2-2**). Albedo returns to ground levels (~0.2) when SAG happens, of which SBSP more often has a later SAG date than SASP. When melt starts to occur, the albedo is highly dependent on new snowfall with rapid albedo decay that follows new snowfall events (**Figure 2-2**). A snowpack that receives no snowfall during times of melt rapidly decays, as the grains are both rounding and growing, while the dust layers are starting to re-emerge. A measurable amount of new snow depth during this time of decay leads to large spikes in albedo (**Figure 2-2**). However, due to the low albedo of the underlying snow, these albedo spikes from new snow decay fast and new snow albedo values decrease to underlying snow albedo values within a day.

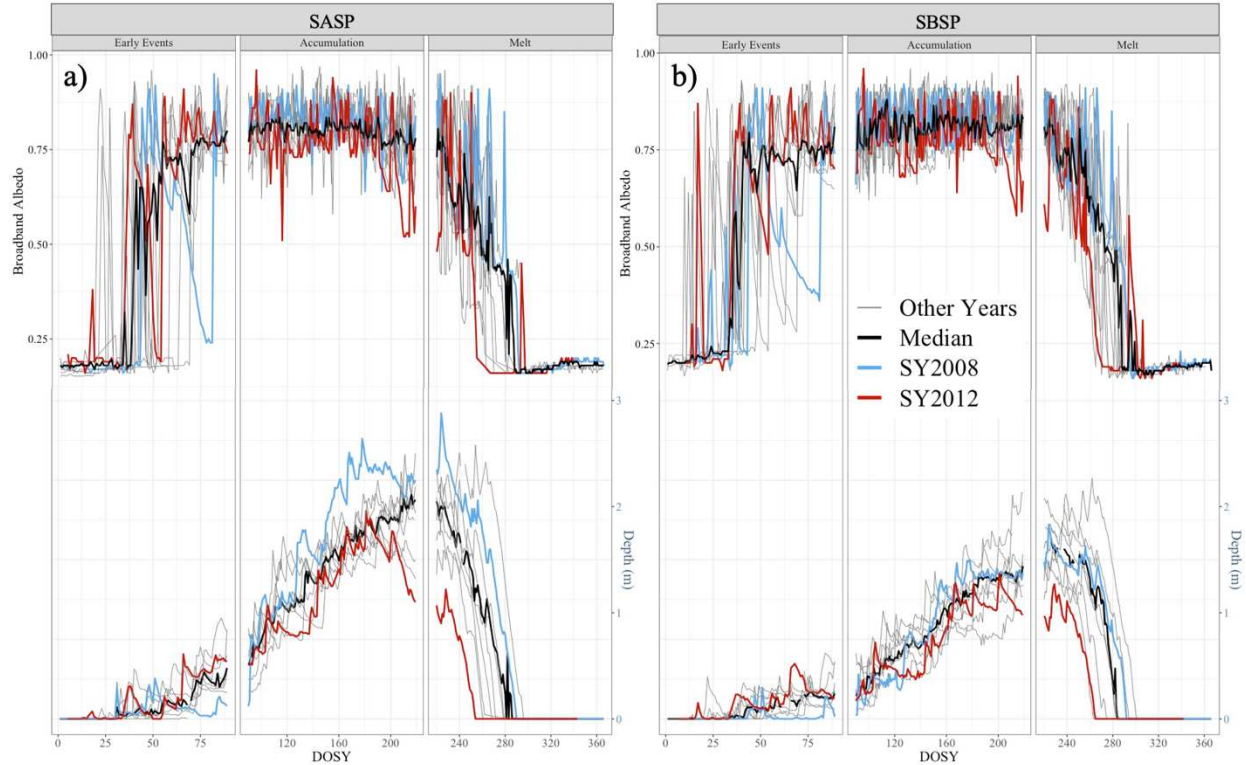


**Figure 2-2.** Daily observed solar noon broadband albedo versus depth values for all nine years, including the median value and highlighting the driest year (SY2012) and wettest (SY2008) at a) Swamp Angel (SASP) and b) Senator Beck (SBSP) Study Plots.

#### 2.4.2. Data Evaluation

There was limited correlation between any of the fresh snow density equations (Appendix A) and albedo values (**Figure 2-3**). The Hedstrom and Pomeroy formulation assumed snowfall only when temperatures were colder than zero degrees Celsius; including temperatures warmer than zero could greatly overestimate density ( $>500 \text{ kg/m}^3$ ). Diamond-Lowry (**Figure 2-3a**) and LaChapelle (**Figure 2-3c**) models both show visual-correlations with albedo but result in an  $R^2$  of 0.03 and an  $R^2$  of 0.04, respectively. The Hedstrom-Pomeroy (**Figure 2-3b**) and particle shape (**Figure 2-3d**) models do not show any pattern with albedo ( $R^2$  of 0.05 and  $R^2$  of 0.00).

However, temperature is the single independent variable describing all four fresh snow density

models, and therefore we do not explore fresh snow density further in this study and use temperature to represent both instead.

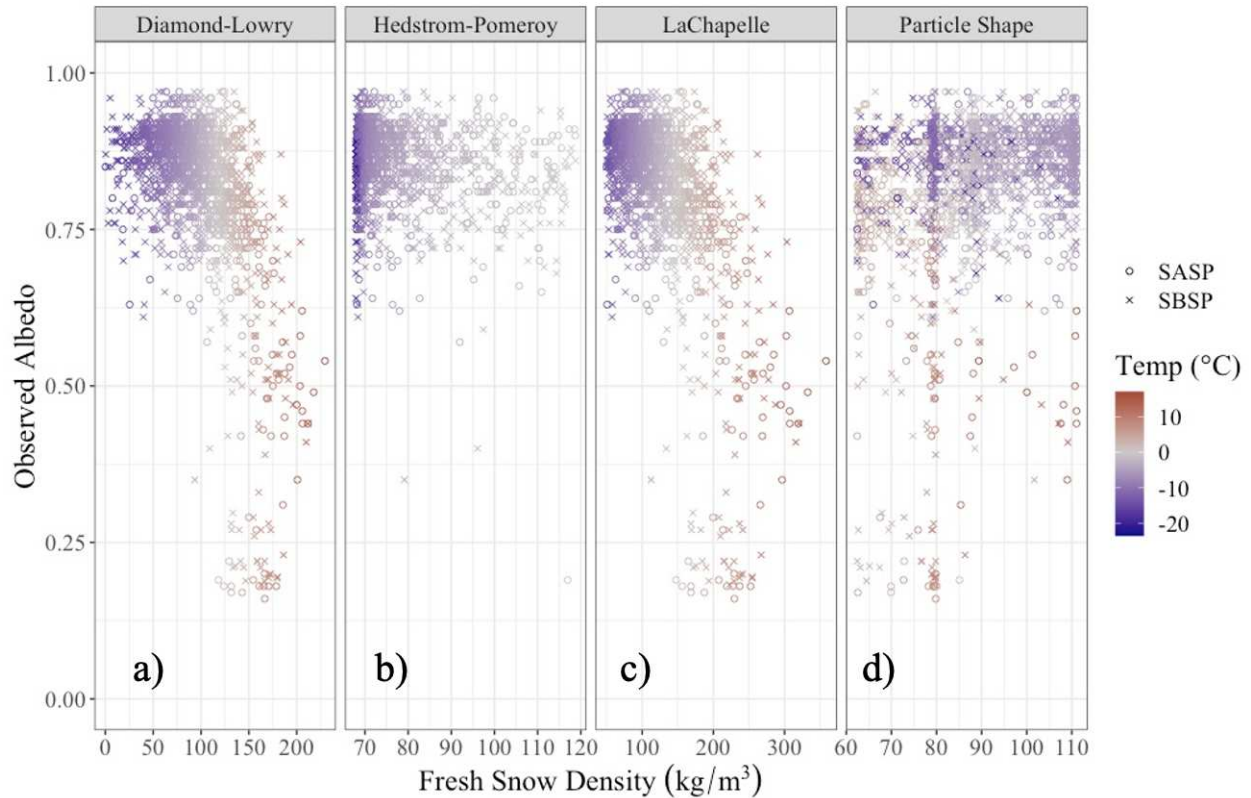


**Figure 2-3.** Fresh snow density of four different models (Appendix A) against observed broadband albedo for both SASP and SBSP. The points are colored by temperature as all four models use temperature as the only variable.

Fresh snow broadband albedo varied widely with temperature, but in general lower albedo values correlated to warmer temperatures and greater fresh snow albedo tended to occur at colder temperatures (**Figure 2-4**). Fresh snow was observed at air temperatures warmer than zero degrees Celsius ( $n = 424$ ), with the warmest temperature of 10 degrees Celsius. At warmer temperatures ( $T \geq 3^\circ\text{C}$ ) fresh snow albedo was highly variable, whereas at colder temperatures there was a smaller range in measured fresh snow albedo (**Figure 2-4**). While the statistical correlation between temperature and broadband albedo was weak ( $R^2 = 0.20$ ), the observed

pattern enabled the use of two temperature bins ( $<3$  versus  $\geq 3^{\circ}\text{C}$ ) in the albedo formulation to separately model each condition.

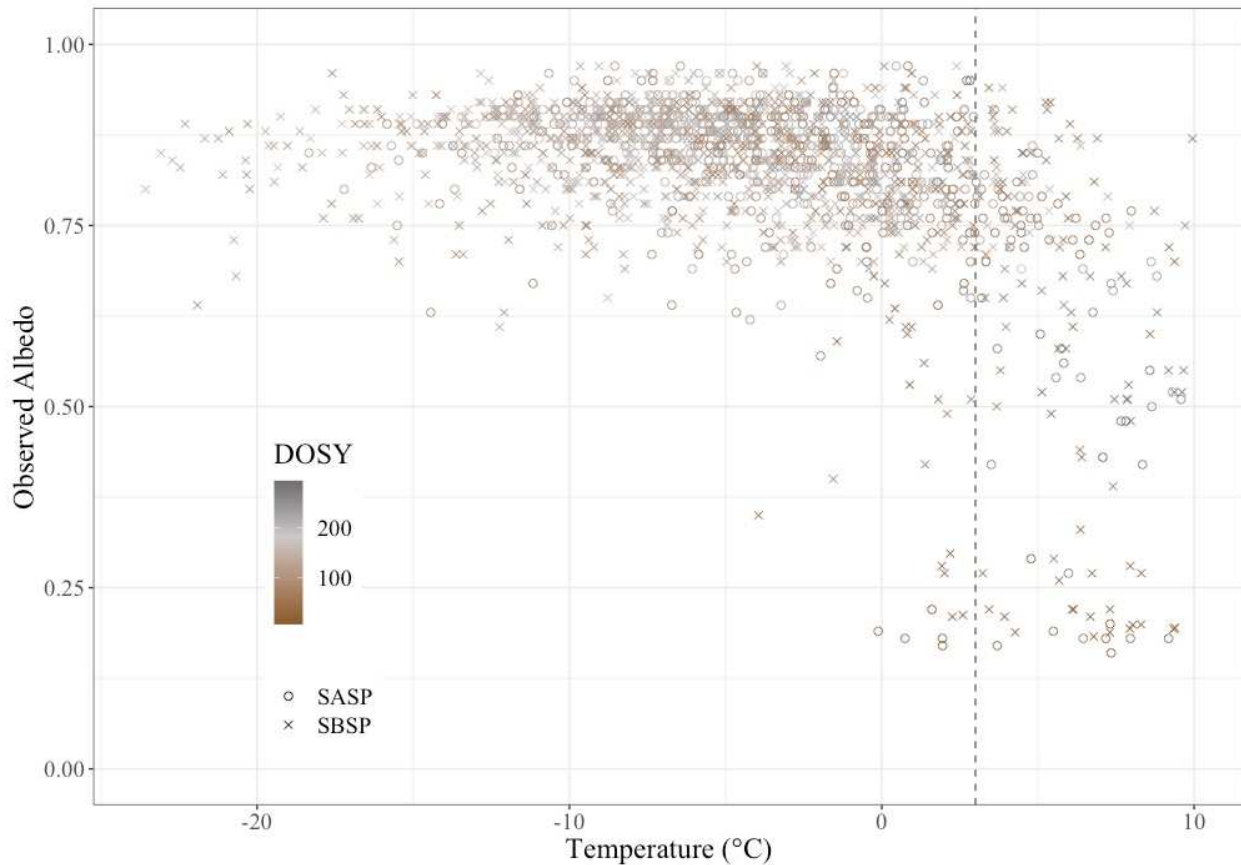


**Figure 2-4.** Temperature plotted with observed broadband albedos for all fresh snow fresh events at the Swamp Angel (SASP) and Senator Beck (SBSP) Study Plots. Points are colored by day of snow year (DOSY), with 1 being September 1 and 365 being August 31 and the dashed vertical line at  $3^{\circ}\text{C}$  shows the temperature threshold for variable fresh snow.

There was no correlation between change in hourly snow depth and fresh snow albedo ( $R^2 = 0.00$ ). During the one-hour time step of the five midday hours, the most frequent snow accumulation was 0.01 meters ( $n = 1106$ ), followed by 0.02 meters ( $n = 334$ ), and then 0.03 meters ( $n = 136$ ). Nine percent of the snow depth increases were deeper than 0.03 meters. There was also a lack of a statistically significant correlation between fresh snow albedo and total snow depth ( $R^2 = 0.09$ ).

### 2.4.3. Estimating Broadband Albedo by Combining Wavelength Groups

A multivariate regression for the visible and NIR-SWIR (NSWIR) wavelength portions of the spectrum was found to accurately calculate broadband albedo (**Figure 2-5**). Using all-snow or the fresh-snow data, the models had the same  $R^2$  and NSE values of 0.99; the regression coefficients deviated little at the 95% confidence interval (**Table 2-3**). The two models had different coefficients for each component of the spectrum (VIS vs. NSWIR) (**Table 2-3**). The all-snow model had a larger coefficient for visible albedo than NSWIR albedo, meanwhile the fresh-snow model had the opposite. Both models also had a minor intercept ( $< \pm 0.03$ ) with the intercept for the fresh-snow model being negative (**Table 2-3**).

**Table 2-3.** Linear model results for both all-snow values and isolated fresh-snow values with a bivariate approach using two wavelength groups, visible and NSWIR albedo, calculated by the pyranometers set up at SBBSA from SY2006-SY2014.

Model	Variables	Coefficients	95% Confidence Interval	Adjusted $R^2$	Degrees of Freedom
All-Snow	Intercept	0.017	(0.017, 0.018)	0.99	44657
	$\alpha_{vis}$	0.526	(0.525, 0.527)		
	$\alpha_{NSWIR}$	0.436	(0.434, 0.438)		
Fresh-Snow	Intercept	-0.025	(-0.031, -0.020)	0.99	862
	$\alpha_{vis}$	0.486	(0.479, 0.493)		
	$\alpha_{NSWIR}$	0.553	(0.545, 0.562)		

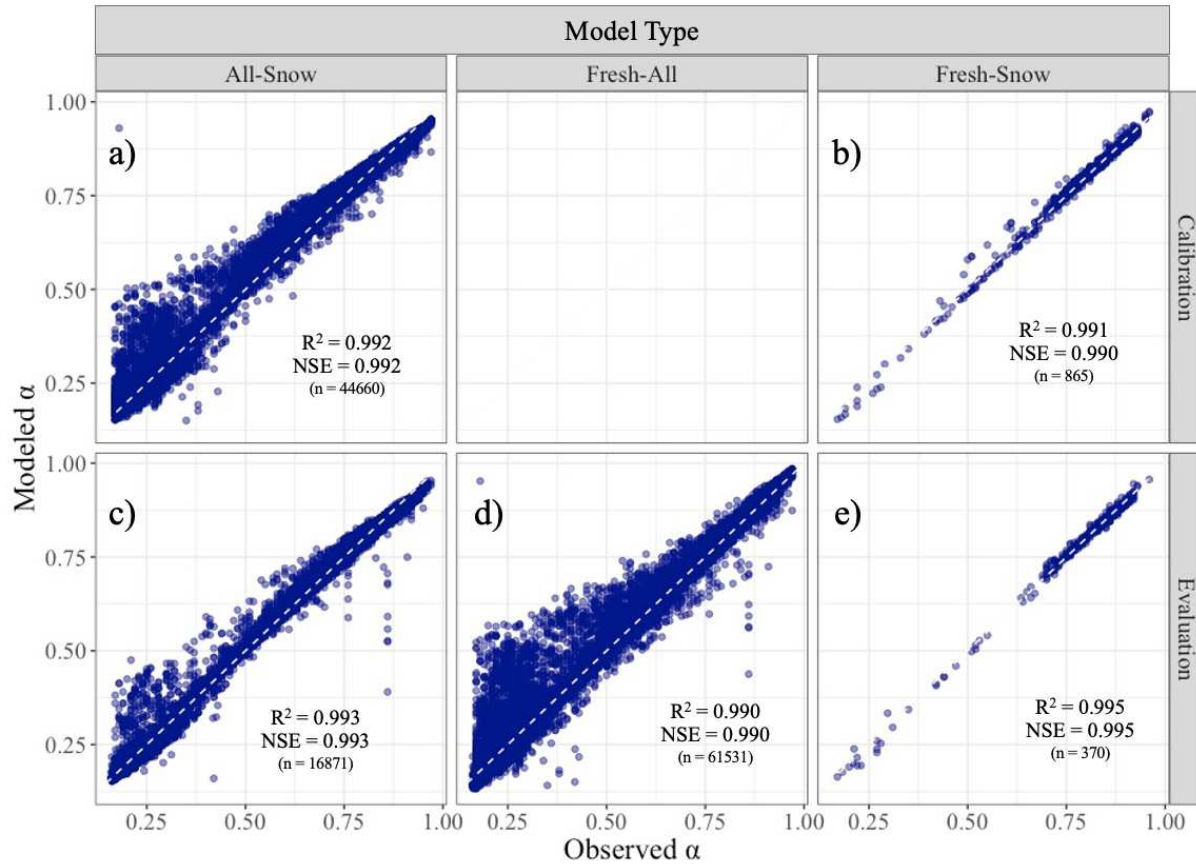


**Figure 2-5.** Observed broadband albedo versus modeled broadband albedo of two models (All-Snow and Fresh-Snow) that used two groups of wavelengths to calculate broadband albedo. The All-Snow model was calibrated (a) and evaluated with all values (c) while the Fresh-Snow model was calibrated (b) and evaluated with both a set of fresh snow values (e) and all snow values (d).

#### 2.4.4. Modeled Fresh Snow Albedo by Multivariate Regression

Dividing the albedo into two wavelength groups, and then recombining each group back into broadband albedo greatly improved the  $R^2$  and NSE values of modeled fresh snow compared to a single broadband albedo model. Without using albedo from the previous time step, nor dividing the albedo into wavelength groups, the NSE was  $<-0.5$ , with  $R^2$  values of less than 0.35 for all models. All of these models used a different combination of meteorological variables (temperature, relative humidity, wind speed), and snow depth. Introducing  $\alpha_{(t-1)}$  improved the model so that the NSE coefficient as 0.77 with an  $R^2$  of 0.81.

Regression modeling fresh snow by the four wavelength and temperature groups, with the same variables as the first round of linear models (including  $\alpha_{(t-1)}$ ), we found the NSE and  $R^2$  values were not that large, specifically for Cold-VIS and Cold-NSWIR (**Table 2-4**). Recombining each wavelength group by temperature to model fresh snow by its respective wavelength, we saw slight increases in accuracy to the visible and NSWIR observed values, (NSE of 0.70,  $R^2$  of 0.78 and NSE of 0.43,  $R^2$  of 0.64, respectively). However, when we recombined the wavelengths back into broadband albedo as the final step using both models in equation 2-3, the all-snow model had an NSE of 0.89 and  $R^2$  of 0.94 while the Fresh-Snow model had an NSE of 0.92 and an  $R^2$  of 0.94 (**Figure 2-6**).

**Table 2-4.** Linear model results for wavelength and temperature groups using meteorological and snowpack multivariate approach. Independent variables came from equipment set up at both plots of SBBSA from SY2006-SY2011.

Model	Variables	Coefficients	95% Confidence Interval	Adjusted $R^2$	Degrees of Freedom
Warm-VIS	Intercept	-0.109	(-0.219, -0.000)	0.84	89
	$\Delta d_s$ (m)	2.494	(-0.298, 5.286)		
	$d_s$ (m)	-0.016	(-0.060, 0.028)		
	$\alpha_{(t-1)}$	1.288	(1.155, 1.421)		
	$T_a$ (°C)	0.009	(-0.003, 0.021)		
	$DE$	-0.002	(-0.010, 0.007)		
Cold-VIS	Intercept	0.215	(0.177, 0.253)	0.64	748
	$\Delta d_s$ (m)	-0.245	(-0.508, 0.017)		
	$d_s$ (m)	-0.001	(-0.009, 0.007)		
	$\alpha_{(t-1)}$	0.864	(0.815, 0.914)		
Warm-NSWIR	Intercept	0.237	(0.183, 0.290)	0.80	123
	$\Delta d_s$ (m)	-0.002	(-0.888, 0.883)		
	$d_s$ (m)	0.011	(-0.003, 0.026)		
	$\alpha_{(t-1)}$	0.580	(0.519, 0.641)		
	$T_a$ (°C)	-0.010	(-0.015, -0.005)		
Cold-NSWIR	Intercept	0.166	(0.125, 0.206)	0.47	1008
	$\Delta d_s$ (m)	0.641	(0.411, 0.871)		
	$d_s$ (m)	0.017	(0.009, 0.026)		
	$\alpha_{(t-1)}$	0.670	(0.617, 0.723)		

For all models, albedo of the previous time step contributed the most to the multivariate regression (**Table 2-4**). Compared to other variables, snow depth and number of dust events had little explanatory power with a narrow range.

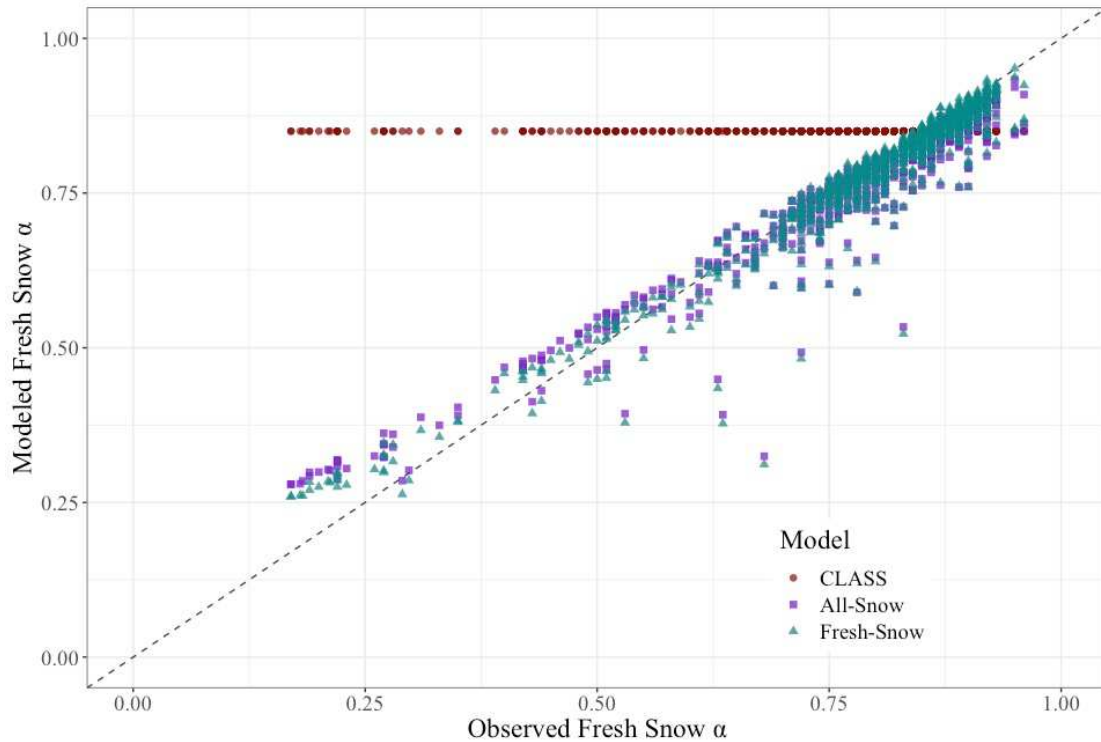


**Figure 2-6.** Observed broadband fresh snow albedo compared to three different fresh snow models of broadband albedo (n=1232), of which CLASS is a static-reset with fresh snow, and the All-Snow and Fresh-Snow vary due to multivariate regression and include measured albedo from the previous time step.

A flow chart of our final methodology is presented in (**Figure 2-7**). The formulation uses a series of decisions to estimate albedo. The first decision is the presence of snow, then an air temperature criterion. If snow is falling, then the albedo is computed as a function of the amount of fresh snow, total snow depth and the albedo from the previous time step. For warmer conditions ( $T \geq 3$  degrees C), temperature is included; in the visible portion of the spectrum the number of dust events is also included. When there is no fresh snow, the albedo decays; it decays at half the rate for colder temperatures.

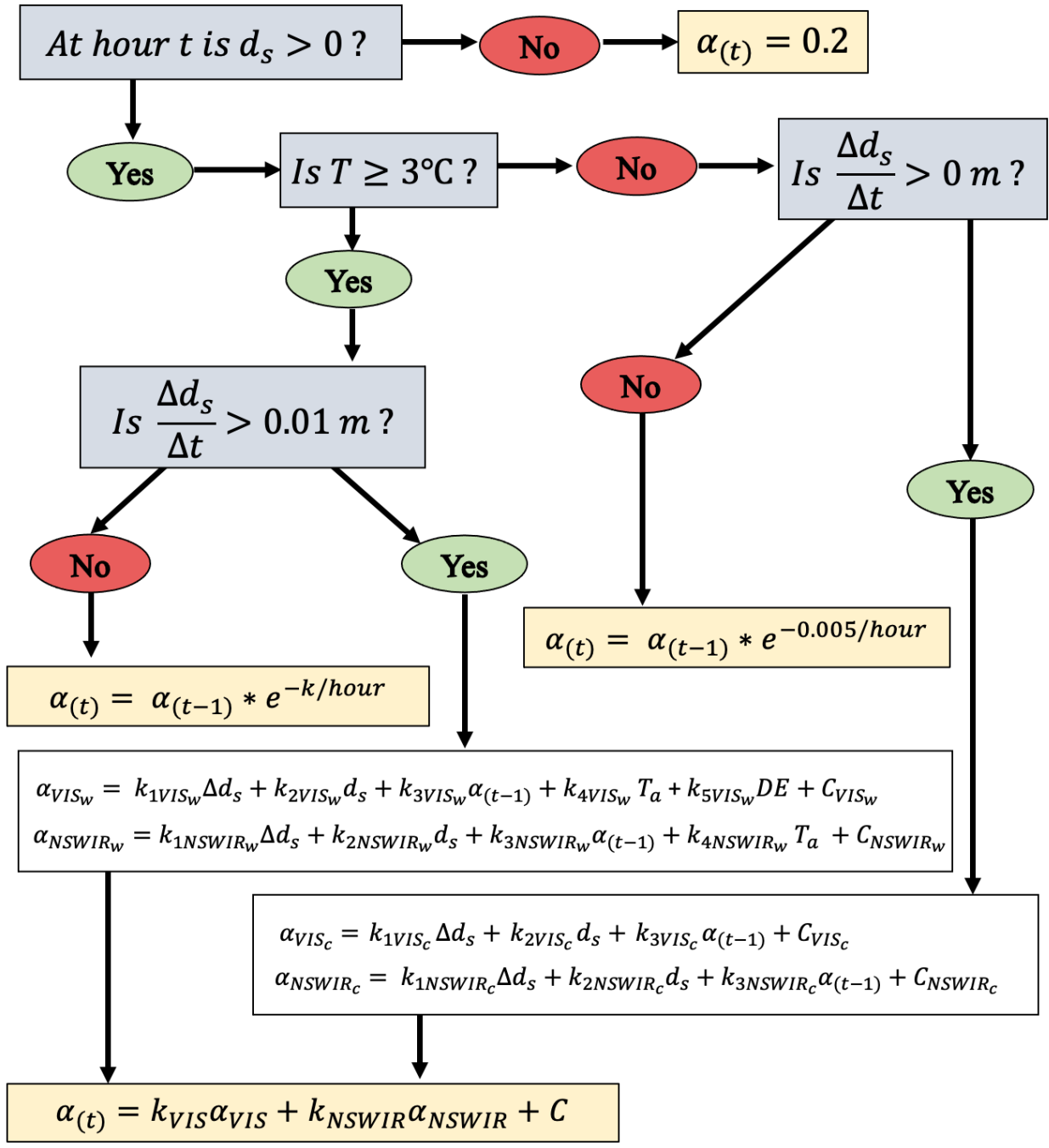


**Figure 2-7.** Flow chart describing the variable fresh snow albedo model. Variables include hourly snow depth ( $d_s$ ), hourly change in snow depth ( $\Delta d_s$ ), albedo from the time step before ( $\alpha_{(t-1)}$ ), number of dust events (DE), and air temperature ( $T_a$ ). Intercepts are represented by  $C$  and coefficients for each variable are represented by  $k_{subscript}$ , with the subscripts referring to the wavelength and temperature group. Where  $w$  is for warm and  $c$  is for cold, VIS is for the visible wavelength group and NSWIR is for near-infrared and shortwave-infrared wavelength group. Albedo decay rates at temperatures greater than  $3^\circ\text{C}$  ( $k$ ) are determined by equation 2-4.

#### 2.4.5. Assessing the Variable Fresh Snow Model

Using the observed albedo from the previous time step to model fresh snow albedo yielded very good results (**Figure 2-6**), but the subsequent albedo decay had decreased accuracy. The final model (**Figure 2-7**) that used all multivariate regression models and two different decay coefficients (**Table 2-4**), without updates from the observed albedo (**Figure 2-6**) produced good results ( $R^2$  of 0.75 and NSE of 0.73), that were an improvement over the CLASS formulation ( $R^2$  of 0.67 and NSE of 0.62) (**Figure 2-8**). There was more variability in the variable fresh snow model, especially for fresh snow albedo, as the CLASS model has an upper limit that is automatically reset when it snows. For both models, a minimum ground albedo was implemented as 0.2, as to not decay albedo to a lower value (**Figure 2-8**). Modeled albedo was more accurate at SBSP than at SASP, based on the  $R^2$  and NSE statistics (**Table 2-5**).

**Table 2-5.** Statistical results from Variable Fresh Snow Model and CLASS compared to observed values at albedo between Swamp Angel Study Plot (SASP), Senator Beck Study Plot (SBSP) and both sites combined. Only daylight albedo values are considered.

Model	Statistic	SASP (n = 27631)	SBSP (n = 31372)	Combined Sites (n = 59647)
Variable Fresh	$R^2$	0.76	0.80	0.75
	NSE	0.73	0.79	0.73
CLASS	$R^2$	0.64	0.72	0.67
	NSE	0.54	0.70	0.62

Full application of the variable fresh snow model showed acceptable statistical correlation for both albedo reset and decay (**Table 2-5**). However, when isolating only the fresh snow albedo values in the variable fresh snow model, computed from modeled albedo from the previous time step, statistical performance dropped ( $R^2$  of 0.46 and NSE of 0.06) (**Figures 2-8b** and **2-8d**). A correlation between CLASS fresh snow albedo values compared to observed cannot

be computed as CLASS fresh snow does not have a standard deviation associated with the static reset value. When isolating non-fresh snow values (i.e., snow that has gone through decay) the variable fresh snow model had an  $R^2$  of 0.76 and NSE of 0.74 and CLASS had an  $R^2$  of 0.67 and NSE of 0.62 (**Figures 2-8a and 2-8c**).

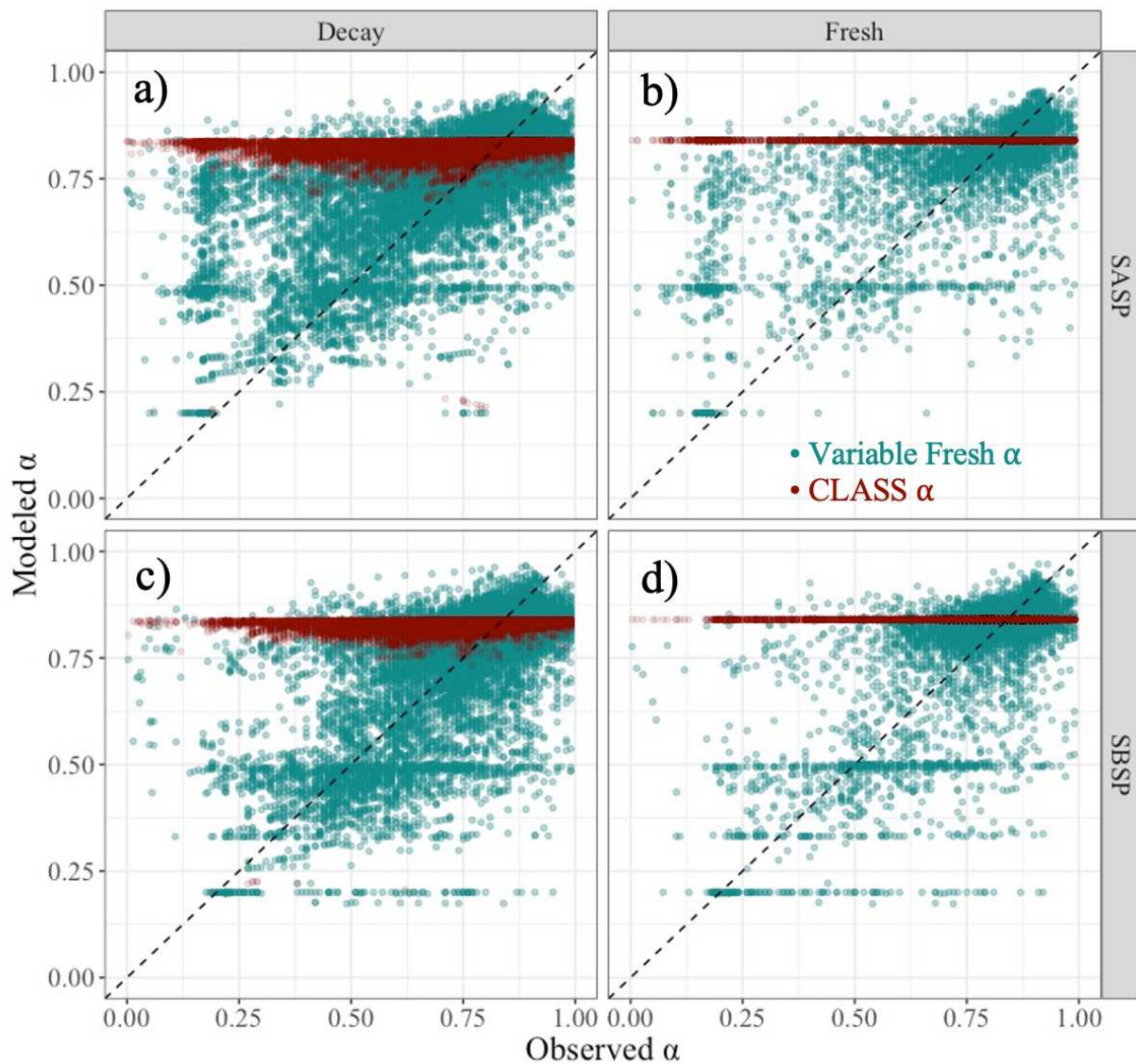


**Figure 2-8.** Observed broadband albedo versus modeled broadband albedo of the variable fresh snow and CLASS albedo models for the Swamp Angel [a) and b)] and Senator Beck [c) and d)] Study Plots. Values have been identified either as fresh snow [b) and d)] ( $\Delta d_s \geq 0.01$  meters) or values where there is no fresh snow and albedo is decaying [a) and c)]

A sequence of early SY2008 and subsequent melt events at SBSP illustrates the contrast between measured and modeled albedo values (**Figure 2-9**). The observed albedo from the pyranometers slowly decayed but did not return to ground albedo levels before the next storm occurred, although snow depth was reported to be zero; measured albedo only increased by more than 0.1 on 10/22 and 11/20 when the measured snow depth increased by at least 0.02 m (**Figure 2-9**). Conversely, when the depth sensors measured no snow depth, this automatically resets CLASS and variable fresh to ground albedo levels. The two albedo models (CLASS and variable fresh) do not compare well with the observed albedo, with the variable fresh model having smaller and more accurate fresh snow albedo values than CLASS (**Figure 2-9**).

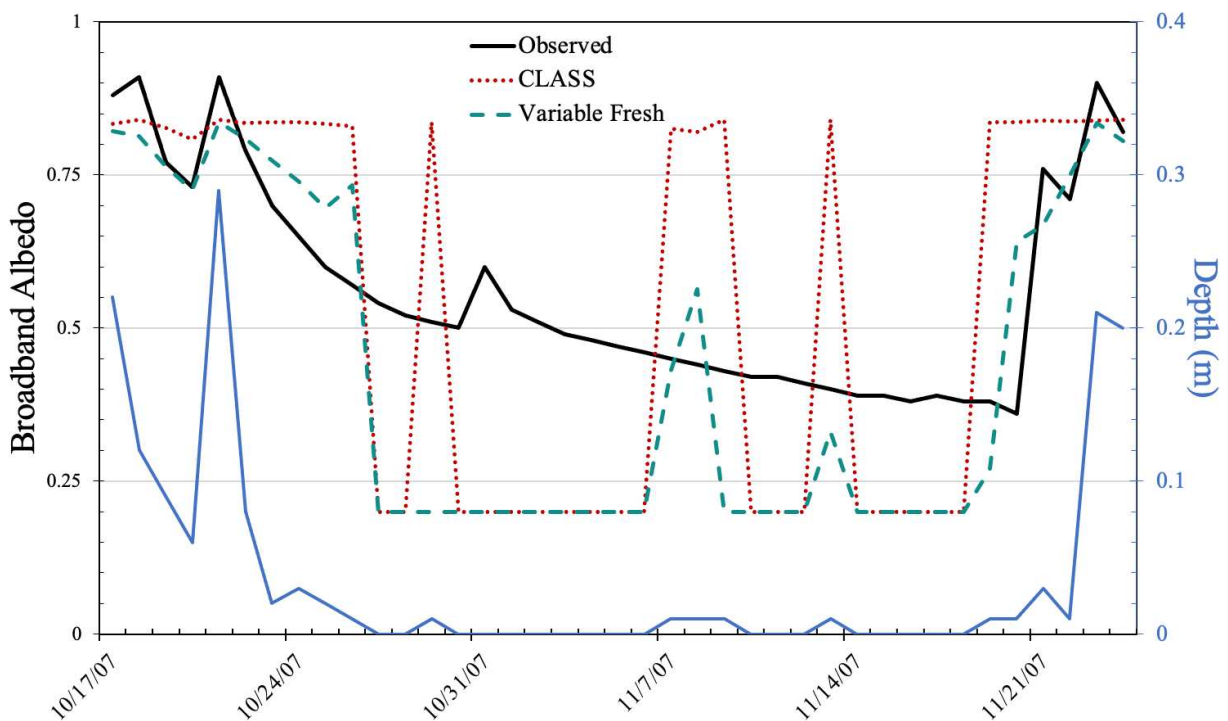


**Figure 2-9.** Solar noon values of modeled broadband albedo and observed albedo with the corresponding depth at Senator Beck Study Plot during the beginning of SY2008.

Late season albedo is lower than albedo the rest of the year (**Figure 2-2**), given the same depth. This is shown by the hysteretic nature of the observed and modeled albedo as a function of snow depth over the season (**Figure 2-10**). Early in the season as snow depth increases, albedo

quickly increases approaching a maximum at about 0.25 meters of depth, then stays consistently high until peak depth about DOSY 200 (~March 19<sup>th</sup>), when both depth and albedo start to decrease, but at a slower rate than its initial increase (**Figure 2-10a**; **Figure 2-10d**). During the accumulation phase of the season, albedo increases with depth are at a lower rate at SASP than SBSP, with more variation (**Figure 2-10a** versus **Figure 2-1-d**). The variable fresh snow model (**Figures 2-10b** and **2-10e**) matches the observed pattern better than CLASS (**Figures 2-10c** and **2-10f**) that tends to remain constant. As snow melts, the albedo decreases in a somewhat linear manner where the variable fresh snow albedo model outperforms CLASS. (**Figure 2-10**). Even though **Figure 2-10** shows the mean albedo results, similar patterns can be seen for each snow year (**Figure B-3**).

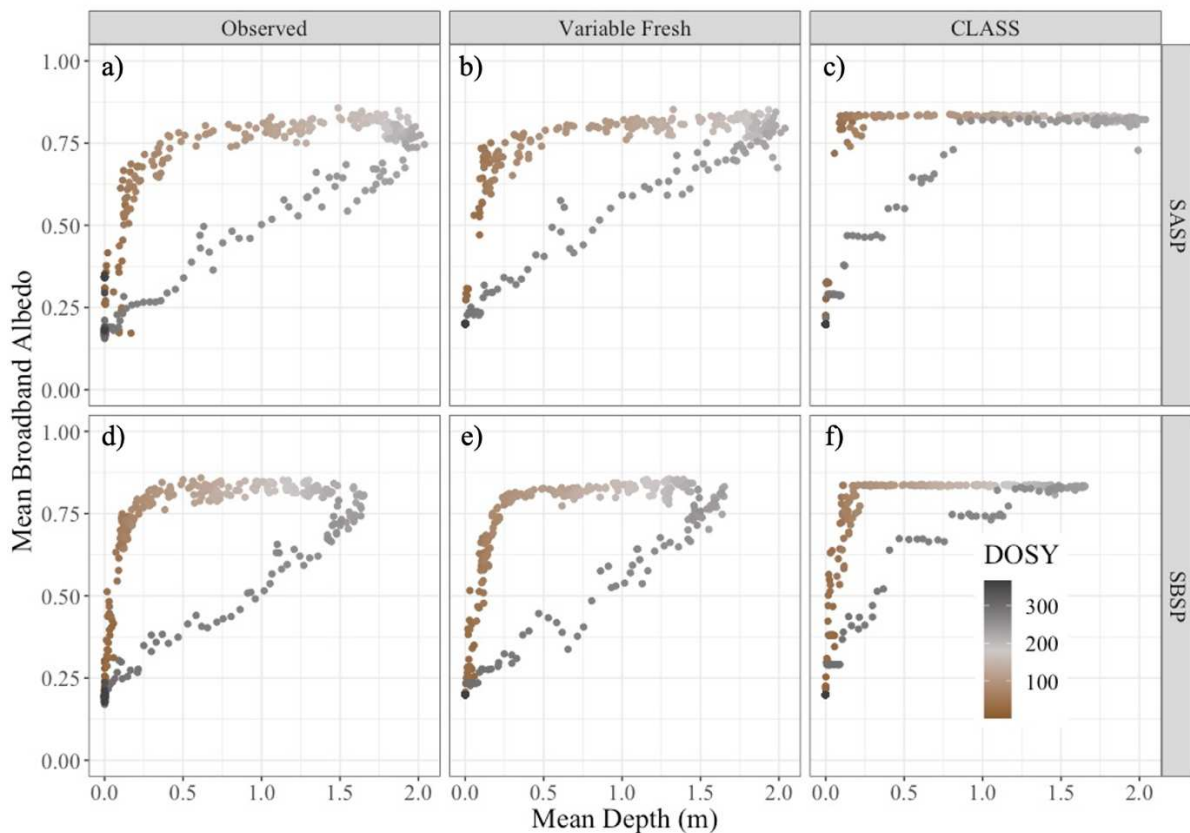


**Figure 2-10.** Mean depth plotted against mean broadband albedo per day for observed values, the variable fresh snow model, and CLASS model for all snow years. Colored by the day (September 1 = DOSY1 and August 31 = DOSY365) separating Swamp Angel (SASP) and Senator Beck Study Plot (SBSP).

On average, net shortwave radiation is underestimated by both models at both sites for the snow season except for the variable fresh snow model for the first events at SBSP (**Figure 2-11a**). Throughout the season, the net shortwave radiation was the least from CLASS (**Figure 2-11**). Except for the outlier noted above, the difference between observed and modeled was consistent for the two sites. During the accumulation portion of the snow season, the differences were the least and the net shortwave radiation was also the least, with the variable fresh snow model being about 10% less than observed and CLASS being about 20% less at SASP (**Figure 2-11b**). The largest differences were during the melt season when the CLASS model estimated only about one-third of the net shortwave radiation compared to the observed, while the variable fresh snow model estimated about two-thirds to three-quarters (**Figure 2-11c**). However, there was much inter-annual variability, as showed by the error bars in **Figure 2-11**. Separating net shortwave radiation into snow year helps show this inter-annual variability (**Figure B-4**).

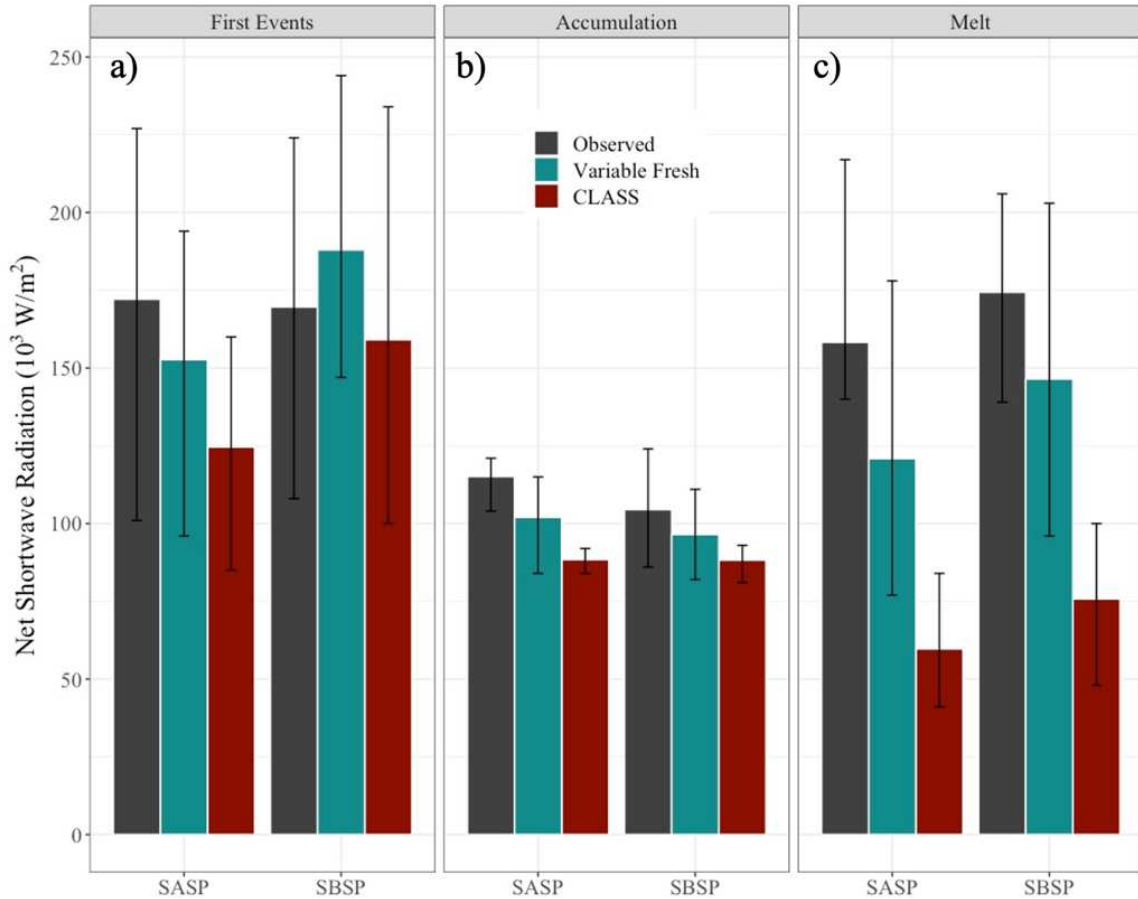


**Figure 2-11.** Mean net shortwave radiation of different seasonal snow timeframes at Swamp Angel and Senator Beck Study Plot for all nine snow years (SY2006-SY2014). Error bars are minimum and maximum absorption for each site for all snow years.

## 2.5. Discussion

### 2.5.1. Quantifying Fresh Snow Albedo

Quantifying the albedo of snow from shortwave radiation measurements can only occur during daylight hours. However, snowfall commonly occurs during the night with some events continuing past sundown and others starting after sundown; snowpack albedo does change without the presence of the sun. Though albedo is irrelevant in the absence of incoming radiation, albedo is an inherent property of the snowpack. When the properties of the snowpack change, even in the absence of the sun, albedo will also change. This is important when trying to

estimate albedo values of the early to mid-morning, which have might have been reset by new snowfall, or possibly decayed, overnight. During winter hours, areas that receive snow are often in darkness for most of the day, which reduces the availability to quantify albedo from pyranometers. When snow falls during the day, the snow depth sensors can only detect change of centimeters per hours and the pyranometers are vulnerable to fluctuations in surface roughness, aspect, and zenith angle. Focusing on values at solar noon is the most consistent timescale that can be used, but it undermines the reality that snow metamorphism is both instantaneous as snow lands on a pack and continuous in the time that follows. The crystalline structures of seasonal snow are ever changing, notably quicker when they first accumulate driven by equilibrium metamorphism from the vapor pressure differences between the convexities and concavities of fresh snow crystals; it slows thereafter (Flanner and Zender 2006). If snow accumulates at night, we can only calculate change in albedo values by reasonable pyranometer measurements from before the snow fell to once the zenith angle is appropriate and the snow is no longer on the upward facing pyranometer. By the time this happens, the fresh snow and the subsurface layers have undergone hours of metamorphism, creating a snow surface with a lower albedo. Additionally, the processes that affect grain metamorphism are also influenced by the radiative transfer of shortwave radiation. When the sun is out, the snow is reflecting most of this radiation, but there is still some radiation that is absorbed and helps drive metamorphism, and possible melting and/or refreezing.

As the sun nears the horizon the albedo of snow increases (Melloh et al. 2002), as is true for most surfaces (Warren 1982). When the zenith angle ( $\theta_z$ ) approaches  $90^\circ$  at dawn and dusk, photons enter the snow system at a grazing angle where the first scattering event happens closer to the surface as compared to when the sky higher in the sky (Warren 1982). This leads to a

higher likelihood of the photon re-emerging by a single-scatter and increasing reflection than if the first scattering were to happen deeper within the snowpack, which leads to multi-scattering and a decreased likelihood of the photon leaving the system. Additionally, snow albedo is more sensitive to zenith angle in the NIR and SWIR wavelengths than the visible, though introductions of impurities would increase the dependence of albedo on zenith angle in the visible spectrum (Warren 1982). Snow does not uniformly distribute reflected radiation into all angles, otherwise snow would be independent of  $\theta_z$ . The angles of reflection are influenced by the bidirectional reflectance properties of snow, often described by grain properties such as the anisotropic reflectance and the geometric asymmetry variables (Bohren and Barkstrom 1974; Warren 1982; Libois et al. 2013), which are complicated properties to model. At increased zenith angles (i.e., when the sun is lower in the sky) the bidirectional reflectance becomes a single-scattering situation where the angle of reflection is highly influenced by the shape of the grain. In contrast, at lower zenith angles, where the bidirectional reflectance continues through the snowpack implying a multiple-scattering situation, the effect from the shape of the snow grains on light reflection becomes more smeared with increased scattering events (Warren 1982). During this time, it is more appropriate to model the snow grains as spheres (Warren 1982). True values of measured albedo need appropriate zenith angles, and this limits the quantity of measurements available for these analyses.

As mentioned previously, snow falling without wind has the potential to collect atop the upward facing pyranometer increasing albedo values by underestimating incoming solar radiation; this can also yield albedo values greater than one. Fortunately, SBSP experiences more wind and since it is relatively close to SASP so that obscured measurements of incoming solar radiation at SASP can be estimated with measured albedo values at SBSP and outgoing

shortwave radiation at SASP (equation 2-1). This adds some level of uncertainty, but it also increases the quantity of data that could be used in this analysis.

### *2.5.2. Late Season Influence on Albedo*

There is an obvious hysteretic correlation between depth and albedo (**Figure 2-10**). During the melt season, for a snow depth that was the same as during the accumulation phase, broadband albedo was less. Thus, using only depth is not enough to estimate broadband albedo of a seasonal snowpack (**Figure 2-10**), nor is only comparing the change in depth to albedo (**Figure B-2**). The characteristics of new snow crystals at the surface and the snow grains and optical properties of the subsurface need to be incorporated into any albedo formulation (Flanner and Zender 2006), yet such detailed information is not readily available. Other surrogate data can be used (**Figure 2-7**).

Regardless of the approach, albedo of the hour was best modeled when the albedo of the previous time step was used (**Table 2-3**), as the two are strongly correlated. For example, during the melt season the albedo during snowfall was much lower than albedo during the early events and accumulation seasons (**Figure 2-2**) due to the lower albedo of the underlying snow and the possible presence of dust (Painter et al. 2012; Skiles et al. 2012). The variable fresh snow model uses temperature as the proxy and can help differentiate the accumulation versus melt seasons for a continental snowpack, such as at SBBSA. Since temperature is the most common measurement at a meteorological station, this is a simple way to define seasonal shifts.

Two factors contributing to the seasonal change in albedo are the surface and subsurface properties. First, in times of new snowfall, the warm temperatures create “wet” spring snow that still increases snow albedo as it accumulates. However, snow albedo quickly decreases right after accumulation due to the snow grain’s vulnerability to melt and the introduction of water, as

well as their less complex shape that reflect less than their supersaturated, cold, accumulating snow crystals (Libbrecht 2005). Secondly, the underlying snow during this time also has a lower albedo than earlier in the season, as the snowpack has aged and the snow grains have become larger, rounder, and the snowpack is denser with less crystalline structure near the surface. New snowfall during times of melt will increase snowpack albedo, but albedo decays rapidly during this time as well. It is important to note that during the melt season, the reflection properties of the surface of the snowpack greatly influences the snowpack albedo. For example, if less radiation enters the snowpack at the surface, due to highly reflective snow grains in the upmost layer, less radiation will penetrate the snow medium, and the albedo will be large. This happens during the accumulation phase when the underlying snow is slowly going through metamorphism and the grains are still relatively new and less dense. Conversely, if less incoming radiation is reflected at the surface, more will penetrate the snow medium, increasing the likelihood of absorption. This happens during the melt phase, when both the surface snow grains, and underlying snow grains are less reflective and more absorptive.

Moreover, as the snowpack becomes more dense and snow depth also decreases, the distance between a dust layer and the snow's surface decreases during melt (Duncan 2020), even if the dust layers remain below the surface until SAG. As the depth between the surface and LAP layer decreases, the multiple-scattering opportunities of the shortwave radiation and the chances for absorption by the dark layer increases. More light can arrive to these internal dust layers due to the shorter path needed for the radiation to reach the dust with less snow depth. Thus, late season albedo is typically less than early season or accumulation season albedo patterns (**Figure 2-2**) necessitating an albedo model to accommodate all time frames. The variable fresh snow

model showed much improved results compared to CLASS values and even showed similar hysteresis patterns to the observed values when compared to depth (**Figure 2-10**).

Whether by larger particles, increased influence from dust layers, affect from the “background” as described by Malik et al. (2015), or some combination thereof, the subsurface of a snowpack is relevant to the albedo of the snow (Thomas 1962; Mellor 1977). Without using a seasonal variable such as bulk density or day of snow year makes it difficult to quantify snow albedo as other variables, such as depth, temperature, or even change in depth, do not describe crystal shape and size at the surface below. Hence using albedo from the previous time step can account for the seasonal changes that bulk density or time would add.

### *2.5.3. Limits and Uncertainties in the Variable Fresh Snow Albedo Model*

Like most models, there are errors associated with estimates. Data from automated sensors inherently have their own measurements of uncertainty that can prorogate through any model (Hultstrand and Fassnacht 2018). The coefficient for change in depth had the largest range of uncertainty using the 95% confidence interval for all four components (**Table 2-4**).

Understanding the limitations of measurements from the ultrasonic depth sensors (Ryan et al. 2008) illustrates the larger error bars associated with change in depth when modeling albedo. Change in depth was sensitive to 0.01 meter for cold temperatures ( $<3^{\circ}\text{C}$ ) and needed to be greater than 0.01 meter for fresh snow to be used in the warmer temperature conditions (**Figure 2-7**). Filtering the data to snow depth increases greater than 0.01 meters would have more than halved the available data (1232 to 487 values for visible and 1654 to 604 values for NSWIR). Even with nine snow-years of data and initially 168,360 observations, only 0.73% of these observations were used to develop the model.

The CLASS or the Variable Fresh Snow model formulation needs an estimate of the surface or ground albedo as a starting point (**Figure 2-7**), and the depth of any new snow. The former can be estimated from land cover type and previously published measurements of albedo (e.g., Oke 1987). The latter can be obtained using a snow depth sensor, but this must consider the uncertainty, as mentioned above. For example, there were times the depth sensors recorded no snow depth (13 days during the period shown in **Figure 2-9**), however the measured broadband albedo was higher than ground albedo, implying some reflection more than the bare ground, or error with pyranometer. without other *in-situ* observations, it is difficult to conclude if there was snow or not, even just a few centimeters.

The uncertainty associated with measured depth can be reduced by using other technologies, in particular non-sonic depth sensors. For example, the laser-based depth sensors (e.g., [lufft.com](http://lufft.com)) are said to measure to the nearest millimeter and not influenced by weather conditions or temperatures. Commercially, such depth sensors are twice the price of the common Ultrasonic Distance Rangers used at meteorological stations, including the Snow Telemetry network, but they would provide increased accuracy when quantifying smaller changes in snow depth, possibly at finer time scales. New inexpensive sensor technology is further reducing the cost of measurement (Ham et al. 2015; Lettenmaier 2017).

The CROCUS snowpack model uses three shortwave radiation wavelength classes to model albedo as a function of grain size: visible, NIR, and SWIR (Brun et al. 1992; Vionnet et al. 2012). The Variable Fresh Snow model keeps visible shortwave radiation separate and combines the NIR and SWIR portions of the spectrum (**Figure 2-7**), since these data are available from the instrumentation at SBBSA (**Table 2-1**). However, these data are not necessary for the model, and reflect different physical processes in different portions of the shortwave

radiation spectrum. The two portions of the shortwave spectrum are estimated separately then combined at the end of each time step. This is similar to the separation of soil variables for snow covered versus snow free areas but then comminated to compute net latent and sensible heat fluxes (Fassnacht and Soulis 2002).

#### *2.5.4. Suggested Improvements for Estimating Fresh Snow Albedo*

Only the number of dust on snow events accumulated through the snow year was included in the model, with the largest effect on the visible portion of albedo (Painter et al. 2007) from dust events occurring in the late season; dust would not affect albedo prior to the first dust. The variable fresh snow model combines variables into one regression, and thus the snowpack is treated only as two layers (Verseghy 1991): the new snow that falls during a time step and the snowpack below. This is analogous to mixing all the layers of the snow into a homogeneous medium; individual dust layers could be considered separately. Other models (e.g., SNTHERM Jordan 1991; CROCUS Brun et al. 1992 and Vionnet et al. 2012) use many different layers of snow, but in many cases the simple two layer snow model is sufficient (Jin et al. 1999). In the San Juan mountains, aeolian dust will deposit on the snow and will soon be covered when snow accumulates over it. These dust events however maintain their integrity as a layer through the snow season and combine with other dust layers near the surface during melt that will compound albedo decay (Skiles and Painter 2018). For increased accuracy, dust needs to be treated different than a numbered event that over-simplifies the complex optical properties associated with these dust layers. We argue that the porous properties of snow drive the multiple-scattering events that creates high albedo, however dust layers below the surface more often absorb the radiation than reflect or transmit, which ends the path of some photon for it to never re-emerge from the snow's surface, this explains why LAPs lower broadband albedo and can decrease the depth of light

penetration in a snowpack (Reay et al. 2012). Not only will this dust layer warm the surrounding snow by radiative transfer and conductive forces from dust to snow, but it will also increase the locations for absorption of the shortwave radiation within the snowpack and lower albedo.

Other metrics of dust could be considered. Through the Colorado Dust-on-Snow program <codos.org>, CSAS also measures the amount of dust in the snowpack, but this is not for individual events; such data could be incorporated into the model. However, pyranometers are not yet common at meteorological stations, nor are specific measurements of dust. More physically-based dust measurements, including concentrations of dust, thickness of dust layers, and dust layer depth relative to the surface, could be useful in better representing dust in an albedo model; we did not have access to consistent measurements for multiple snow years of such properties. Including the number of dust events did increase the accuracy of albedo for visible wavelengths, but the correlation was weak (**Table 2-3**). Numerous papers provide evidence of LAPs affecting albedo (e.g., Painter et al. 2012; Skiles et al. 2012; Gleason and Nolin 2016), and we can emphasize the need to incorporate LAP concentrations into albedo decay to accelerate melt. This model only used dust levels to vary fresh snow albedo values, not to vary decay (**Figure 2-7**); we encourage model users to adjust albedo decay rates accordingly (Bryant et al. 2013).

The variable that influences the calculation of fresh snow albedo the most was of albedo from the previous time step (**Table 2-4**). This value, however, was dependent on the albedo decay rate. The accuracy of modeled compared to the observed fresh snow when albedo using observed  $\alpha_{(t-1)}$  was exceptional (NSE and  $R^2 > 0.99$ ), as expected. Improving modeled  $\alpha_{(t-1)}$  values by representative albedo decay rates would thus increase in the model accuracy. While this model is not perfect for estimating albedo for an entire snow year (**Figure 2-10**), it is an

improvement on the original CLASS formulation, especially during melt (**Figure B-3**), and more simple than models such as SNICAR (Flanner and Zender 2006), CROCUS (Brun et al. 1992; Vionnet et al. 2012), and the Alpine and Sub-Alpine albedo model (Melloh et al. 2002). This model can provide reasonable fresh snow albedo results, given representative decay rates (Flanner and Zender 2006).

## 2.6. Conclusion

We set out to quantify the broadband albedo of fresh snow using automated sensor data from two high-elevation study plots in the San Juan Mountains. We found that fresh snow albedo could not be predicted by any single variable, but instead a multivariate approach that used snow depth, change in snow depth, temperature, albedo from the timestep before, and number of dust events that exist within the snow. Furthermore, fresh snow albedo was better described when grouped by temperature using a threshold of three degrees Celsius and by grouping into two different wavelength groups, visible and near-shortwave infrared. The model uses few variables that are measured at some meteorological stations or included in other models, specifically snow depth, temperature, an estimation of ground albedo, and though optional due to its weak correlation, a count of aeolian dust deposition events that is mostly relevant in late season.

Snow albedo, both of fresh and decaying snow, is complicated and difficult to model due to the dynamics associated with individual crystals and grains through the surface and subsurface of a snowpack that affect the cumulative optical properties of the medium. Bulk estimates of the snowpack, such as depth and density, do not describe measurements of albedo nearly as well as using physical assumptions, like using temperature to describe snow crystal integrity, or wavelength groups to describe spectrally unique reflection. The variable fresh snow model uses

niveometeorological variables and groups by temperature and wavelength to best describe the physical nature of the shortwave reflectance properties for a seasonal snowpack.

## CHAPTER 3. IMPLICATIONS

The variable fresh snow model is different than many models as it starts from the ground-up using the albedo of the ground. This value can be assumed based on land cover and could be the only required albedo value as a basis for the first snow event. Models that reset snow albedo to a static value treat fresh snow albedo as a parameter rather than a variable, which it is. Such models treat albedo as a function of the surface, not incorporating the complex optical behavior of the subsurface properties for either fresh snow or decay. This can greatly affect both the quantity of shortwave radiation that will exit the snow surface and the amount that is absorbed through the snow system. Neither depth or density can accurately describe albedo for an entire season, as these are only bulk estimates of the snowpack and a deep seasonal snowpack shows variable albedo per snow depth and uncertainty in albedo values for bulk and fresh snow density. During early season events and accumulation, depth versus albedo results were comparable to the findings of Burakowski et al. (2015) that saw a logarithmic increase in albedo with increased depth. In contrast, the albedo during the melt of a seasonal snowpack was not on the same logarithmic curve as the early season. It decayed more linearly and rapidly. Seasonal snowpacks of Colorado have different characteristics than those of New Hampshire and the Northeastern United States (where the Burakowski et al. 2015 occurred), especially that the snow depth is shallower.

The optical properties of individual snow crystals and grains, the angle at which the shortwave radiation penetrated the snow, any light absorbing particles along the path of some photon, and how these variables interact all influence albedo. Any reflection, absorption, or transmittance of a photon happens at and through the ice-air or ice-ice interface of individual

particles or is absorbed by a dust layer, especially when the dust layers combine in late season melt. The best way to measure and model snow albedo, is with a physical approach, using variables that influence and hopefully describe the complex processes involving shortwave radiation and ever-changing snow grains.

Calculating the optical properties of the fresh and subsurface snow, such as SSA, anisotropic reflectance, and the geometric asymmetry variables, is complicated, so that snow particles are often only represented as spheres or equivalents thereof. Snow grains round with age, and an optically equivalent sphere is a more appropriate shape when describing older snow below the surface, yet not for snow that is faceted. Conversely, fresh snow crystals at cold temperatures can be dendritic, highly reflective, and vulnerable to rapid decay given any change in environmental conditions; these can be misrepresented when considered as spheres. Increases in depth at an hourly time scale and during small zenith angles had a weak correlation when estimating albedo. During the shoulder seasons of low depth, albedo did not always reset to some maximum value, regardless of the change in depth, as albedo is affected by other variables.

Like most hydrologic computations, there will be uncertainty in the equipment, noise from the environment, and discrepancies in the values regardless of the complexity and completeness of the model. We present the variable fresh snow albedo model that shows high accuracy in albedo values during times of fresh snow when the albedo of the previous time step is also accurately estimated. This model works best in juxtaposition with variable decay coefficients that are dependent on variables that better represent the physical nature of the light reflecting properties of snow crystals and snow grains.

## REFERENCES

- Bales, R.C., R.E. Davis, and D.A. Stanley (1989). Ion Elution Through Shallow Homogenous Snow. *Water Resources Research* 25(8): 1869-1877. DOI: 10.1029/WR025i008p001869
- Barnett, T.P., J. C. Adam, and D.P. Lettenmaier (2005). Potential impacts of a warming climate on water availability in snow-dominated regions. *Nature* 438(7066): 303-309. DOI: 10.1038/nature04141
- Bergen, J.D. (1970). A possible relation between grain size, density, and light attenuation in natural snow cover. *Journal of Glaciology* 9(55): 154-156. DOI: 10.3189/S0022143000026915
- Bohren, C., and B. Barkstrom (1974). Theory of Optical Properties of Snow. *Journal of Geophysical Research* 79(30): 4527-4535. DOI: 10.1029/JC079i030p04527
- Brandt, R.E., S.G. Warren, A.P. Worby, and T.C. Grenfell (2005). Surface Albedo the Antarctic Sea Ice Zone. *Journal of Climate* 18(17): 3606-3622. DOI: 10.1175/JCLI3489.1
- Brun, E., P. David, M. Sudul, and G. Brunot (1992). A numerical model to simulate snow-cover stratigraphy for operational avalanche forecasting. *Journal of Glaciology* 38(128): 13-22. DOI: 10.3189/S0022143000009552
- Bryant, A.C., T.H. Painter, J.S. Deems, and S.M. Bender (2013). Impact of dust radiative forcing in snow on accuracy of operational runoff prediction in the Upper Colorado River Basin: DUST IN SNOW IMPACT ON STREAMFLOW. *Geophysical Research Letters* 40(15): 3945-3949. DOI:10.1002/grl.50773
- Burakowski, E., C.P. Wake, J.E. Dibb, and M. Stampone (2013). Putting the capital 'A' in CoCoRAHS: an experimental programme to measure albedo using the Community Collaborative Rain, Hail & Snow (CoCoRaHS) Network. *Hydrological Processes* 27: 3024-3034. DOI: 10.1002/hyp.9825
- Colbeck, S.C. (1980). Thermodynamics of snow metamorphism due to variations in curvature. *Journal of Glaciology* 26(94): 291-301. DOI: 10.1017/S0022143000010832
- Diamond, M., and W.P. Lowry (1953). Correlation of density of new snow with 700 mb temperature. Snow, Ice, and Permafrost research Establishment, SIPRE Research Paper 1, Corps of Engineers, Wilmette IL.
- Doskocil, L.G., S.R. Fassnachy, and J.E. Derry, *in review*. Mystery Peaks: Estimating the Unusual Double Peak Streamflow Behavior in the Uncompahgre River Basin. Colorado Water (submitted 2021).

Duncan, C.R. (2020). Patterns of dust-enhanced absorbed energy and shifts in melt timing for snow of Southwestern Colorado. Unpublished M.S. thesis, Watershed Science, Colorado State University, Fort Collins, Colorado, USA, 53 pp + 3 Appendices (57 pages total).

Dunkle, R.V., and J.T. Bevens (1956). An Approximate Analysis of the Solar Reflectance and Transmittance of a Snow cover. *Journal of Meteorology* 13: 212-216.

Fassnacht, S.R., K.R. Snelgrove, and E.D. Soulis (2001). Daytime incoming longwave radiation approximation for physical hydrological modelling. Soil-Vegetation-Atmosphere Transfer Schemes and Large-Scale Hydrological Models (Proceedings Sixth IAHS Scientific Assembly Symposium S5, Maastricht, July 2001), IAHS, 270, 279-286.

Fassnacht, S.R., and E.D. Soulis (2002). Implications during transitional periods of improvements to the snow processes in the Land Surface Scheme – Hydrological Model WATCLASS. *Atmosphere-Ocean*, 40(4): 389-403.

Fassnacht, S.R., M.W. Williams, and M.V. Corrao (2009). Changes in the surface roughness of snow from millimetre to metre scale. *Ecological Complexity* 6(3): 221-229. DOI: 10.1016/j.ecocom.2009.05.003

Fischer, A.P. (2011). The Measurement Factors in Estimating Snowfall Derived from Snow Cover Surface Using Acoustic Snow Depth Sensors. *Journal of Applied Meteorology and Climatology* 50: 691-699. DOI: 10.1175/2010JAMC2408.1

Flanner, M.G., and C.S. Zender (2005). Snowpack radiative heating: Influence on Tibetan Plateau climate. *Geophysical Research Letters* 32(6): L06501. DOI: 10.1029/2004GL022076

Flanner, M.G., and C.S. Zender (2006). Linking snowpack microphysics and albedo evolution. *Journal of Geophysical Research* 111: D12208. DOI: 10.1029/2005JD006834

Gleason, K.E., and A.W. Nolin (2016). Charred forests accelerate snow albedo decay: parameterizing the post-fire radiative forcing on snow for three years following fire. *Hydrological Processes* 30: 3855-3870. DOI: 10.1002/hyp.10897

Gray, D.M., and P.G. Landine (1987). Albedo model for shallow prairie snow covers. *Canadian Journal of Earth Science* 24: 1760-1768. DOI: 10.1139/e87-168

Grenfall, T.C., and G.A. Maykut (1977). The optical properties of ice and snow in the Arctic Basin. *Journal of Glaciology* 18: 445-463. DOI: 10.1017/S0022143000021122

Ham, J.M., G.L. Miner, and G.J. Kluitenberg (2015). A New Approach to Sap Flow Measurement Using 3D Printed Gauges and Open-source Electronics. American Geophysical Union Fall Meeting, San Francisco California USA, December 2015; abstract number H32B-04.

Hedstrom, N. and J.W. Pomeroy (1998). Measurements and modelling of snow interception in the boreal forest. *Hydrological Processes* 12: 1611-1625.

- Hultstrand, D.M. and S.R. Fassnacht (2018). The sensitivity of snowpack sublimation estimates to instrument and measurement uncertainty perturbed in a Monte Carlo framework. *Frontiers of Earth Science* 12(4): 728-738. DOI: 10.1007/s11707-018-0721-0
- Jin, J., X. Gao, Z.-L. Yang, R.C. Bales, S. Sorooshian, R.E. Dickinson, S.F. Sun, and G.X. Wu (1999). Comparative Analyses of Physically Based Snowmelt Models for Climate Simulations. *Journal of Climate* 12(8): 2643-2657.
- Jonsell, U., R. Hock, and B. Holmgren (2003). Spatial and temporal variations in albedo on Storglaciären, Sweden. *Journal of Glaciology* 49(164): 59-68. DOI: 10.3189/172756503781830980
- Jordan, R. (1991). A one-dimensional temperature model for a snow cover: technical documentation for SNTHERM. 89. U.S. Army Corps of Engineers, Cold Regions Research and Engineering Laboratory. 29 pp.
- LaChapelle, E.R. (1961). *Snow Layer Densification*. Alta Avalanche Study Center, Project F, Progress Report No. 1, Us Department of Agriculture Forest Service, Wasatch National Forest, 8 pp.
- Landry, C.C., K.A. Buck, M.S. Raleigh, and M.P. Clark (2014). Mountain system monitoring at Senator Beck Basin, San Juan Mountains, Colorado: A new integrative data source to develop and evaluate models of snow and hydrologic processes. *Water Resource Research* 50: 1773-1788. DOI: 10.1002/2013WR013711
- Lettenmaier, D.P. (2017). Observational breakthroughs lead the way to improved hydrological predictions. *Water Resources Research* 53: 2591-2597. DOI: 10.1002/2017WR020896
- Libbrecht K.G. (2005). The physics of snow crystals. *Reports on Progress in Physics* 68: 855-895. DOI: 10.1088/0034-4885/68/4/R03
- Libois, Q., G. Picard, J.L. France, L. Arnaud, M. Dumont, C.M. Carmagnola, and M.D. King (2013). Influence of grain shape on light penetration in snow. *The Cryosphere* 7: 1803-1818. DOI: 10.5194/tc-7-1803-2013
- Liljequist, G.H. (1956). Energy exchange of an Antarctic snow-field: Short-wave radiation (Maudheim 71°03'S, 10°56'W), in *Norwegian-British-Swedish Antarctic Expedition, 1949-52, Scientific Results*, vol. 2, part 1A, Norsak Polarinstitut, Oslo.
- Liston, G., and K. Elder (2006). A Distributed Snow-Evolution Modeling System (SnowModel). *Journal of Hydrometeorology* 7(6): 1259-1276. DOI: 10.1175/JHM548.1
- Malik, M.J., R. van der Velde, Z. Vekerdy, and Z. Su (2014). Improving modeled snow albedo estimates during the spring melt season. *Journal of Geophysical Research: Atmospheres* 119: 7311-7331. DOI: 10.1002/2013JD021344

- Marks, D., and J. Dozier (1992). Climate and energy exchange at the snow surface in the Alpine Region of the Sierra Nevada: 2. Snow cover energy balance. *Water Resource Research* 28(11): 3043-3054. DOI: 10.1029/92WR01483
- Marks, D., J. Domingo, D. Susong, T. Link, and D. Garen (1999). A spatially distributed energy balance snowmelt model for application in mountain basins. *Hydrological Processes* 13: 1935-1959.
- Melloh, R.A., J.P. Hardy, R.N. Bailey, and T. Hall (2002). An efficient snow albedo model for the open and sub-canopy. *Hydrological Processes* 16: 3571-2584. DOI: 10.1002/hyp.1229
- Mellor, M. (1977). Engineering properties of snow. *Journal of Glaciology* 19(81): 15-66. DOI: 10.3189/S002214300002921X
- Munson, S.M., J. Belnap, and G.S. Okin (2011). Responses of wind erosion to climate-induced vegetation changes on the Colorado Plateau. *Proceedings of the National Academy of Sciences of the United States of America* 108(10): 3854-3859. DOI: 10.1073/pnas.1014947108
- Nakamura, T., O. Abe, T. Hasegawa, R. Tamura, and T. Ohta (2001). Spectral reflectance of snow with a known grain-size distribution in successive metamorphism. *Cold Regions Science and Technology* 32: 13-26. DOI: 10.1016/S0165-232X(01)00019-2
- Nash, J.E. and J.V. Sutcliffe (1970). River flow forecasting through conceptual models part I – A discussion of principles. *Journal of Hydrology* 10(3): 282-290. DOI: 10.1016/0022-1694(70)90255-6
- Neff, J.C., A.P. Ballantyne, G.L. Farmer, N.M. Mahowald, J.L. Conroy, C.C. Landry, J.T. Overpeck, T.H. Painter, C.R. Lawrence, and R.L. Reynolds, (2008). Increasing aeolian dust deposition in the western United States linked to human activity. *Nature Geoscience* 1(3): 189-198. DOI: 10.1038/ngeo133
- Oke T.R. (1987). *Boundary layer climates*. Routledge. 464 pp.
- Painter, T.H., M.S. Skiles, J.S. Deems, A.C. Bryant, and C.C. Landry (2012). Dust radiative forcing in snow of the Upper Colorado River Basin: 1. A 6 year record of energy balance, radiation, and dust concentrations. *Water Resources Research* 48: W07521. DOI: 10.1029/2012WR011985
- Picard, G., L. Arnaud, F. Domie, and M. Fily (2009). Determining snow specific surface area from near- infrared reflectance measurements: Numerical study of the influence of grain shape. *Cold Regions Science and Technology* 56: 10-17. DOI: 10.1016/j.coldregions.2008.10.001
- Qu, X., and A. Hall (2007). What Controls the Strength of Snow-Albedo Feedback? *Journal of Climate* 20: 3971-3981. DOI: 10.1175/JCLI4186.1

- Rasmussen R., L. Changhai, K. Ikeda, D. Gochis, D. Yates, F. Chen, M. Tewari, M. Barlage, J. Dudhia, W. Yu, K. Miller, K. Arsenault, V. Grubišić, G. Thompson, and E. Gutmann (2011). High-Resolution Coupled Climate Runoff Simulations of Seasonal Snowfall over Colorado: A Process Study of Current and Warmer Climate. *Journal of Climate* 24(12): 3015-3048. DOI: 10.1175/2010JCLI3985.1
- Reay, H.J., J.L. France, and M.D. King (2012). Decreased albedo, *e*-folding depth and photolytic OH radical and NO<sub>2</sub> production with increased black carbon content in Arctic snow. *Journal of Geophysical Research* 117: D00R20. DOI: 10.1029/2011JD016630
- Ryan W.A., N.J. Doesken, and S.R. Fassnacht (2008). Evaluation of Ultrasonic Snow Depth Sensors of U.S. Snow Measurements. *Journal of Atmospheric and Oceanic Technology* 25(5): 667-684. DOI: 10.1175/2007JTECHA947.1
- Schoennagel T., T.T. Veblan, and W.H. Romme (2004). The Interaction of Fire, Fuels, and Climate across Rocky Mountain Forests. *Bioscience* 54(7): 661-676.
- Skiles, M.S., T.H. Painter, J.S. Deems, A.C. Bryant, and C.C. Landry (2012). Dust radiative forcing in snow of the Upper Colorado River Basin: 2. Interannual variability in radiative forcing and snowmelt rates. *Water Resources Research* 48: W07522. DOI: 10.1029/2012WR011986
- Skiles, M.S., T.H. Painter, J. Belnap, L. Holland, R.L. Reynolds, H.L. Goldstein, and J. Lin (2015). Regional variability in dust-on-snow processes and impacts in the Upper Colorado River Basin. *Hydrological Processes* 29: 5397-5413. DOI: 10.1002/hyp.10569
- Skiles, M.S., and T.H. Painter (2018). Assessment of Radiative Forcing by Light-Absorbing Particles in Snow from In Situ Observations with Radiative Transfer Modeling. *Journal of Hydrometeorology* 19: 1397-1409. DOI: 10.1175/JHM-D-18-0072.1
- Skiles M.S. (2019). Senator Beck Basin with Corrected Radiation (Water Years 2005-2014)(Version 1)[Data set]. *Zenodo*. DOI: 10.5281/zenodo.2532590
- Thomas, C.W. (1962). On the transfer of visible radiation through sea ice and snow. *Journal of Glaciology* 4: 481-484. DOI: 10.3189/S0022143000027921
- US Army Corps of Engineers (1956). *Snow Hydrology: Summary Report of the Snow Investigations*. North Pacific Division, Portland, OR 437p.
- Verseghy, D.L. (1991). Class-A Canadian land surface scheme for GCMS. I. Soil model. *International Journal of Climatology* 11(2): 111-133.
- Vionnet, V., E. Brun, S. Morin, A. Boone, S. Faroux, P. Le Moigne, E. Martin, and J-M. Willemet (2012). The detailed snowpack scheme Crocus and its implementation in SURFEX v7.2. *Geoscientific Model Development* 5: 773-791. DOI: 10.5194/gmd-5-773-2012

Warren, S.G., 1982. Optical Properties of Snow. *Reviews of Geophysics and Space Physics*20(1): 67-89. DOI: 10.1029/RG020i001p00067

APPENDIX A. ADDITIONAL EQUATIONS AND FIGURES

$$\cos(\beta) = \cos(\theta_z) * \cos(\theta_n) + \sin(\theta_z) * \sin(\theta_n) * \cos(\phi_s - \phi_n) \quad [A-1]$$

Where  $\beta$  is the local zenith angle,  $\theta_z$  is the solar zenith angle for the horizontal surface,  $\theta_n$  is the surface slope,  $\phi_s$  is the solar azimuth angle and  $\phi_n$  is the surface aspect (after Painter et al. 2012).

$$M_\beta = \frac{\cos(\beta)}{\cos(\theta_z)} \quad [A-2]$$

Where  $M_\beta$  is the scalar by which to correct measurements of hourly incoming shortwave radiation values to radiation that arrives to the surface (after Painter et al. 2012).

$$\rho_{s_{freshDiamond-Lowry}} = 119 + 6.48 * T_a \quad [A-3]$$

Where  $\rho_{s_{fresh}}$  is the density of fresh snow,  $T_a$  is air temperature in degrees Celsius. After Diamond and Lowry (1953).

$$\rho_{s_{freshLaChapelle}} = 50 + 1.7 * (T_a + 15)^{1.5} \quad [A-4],$$

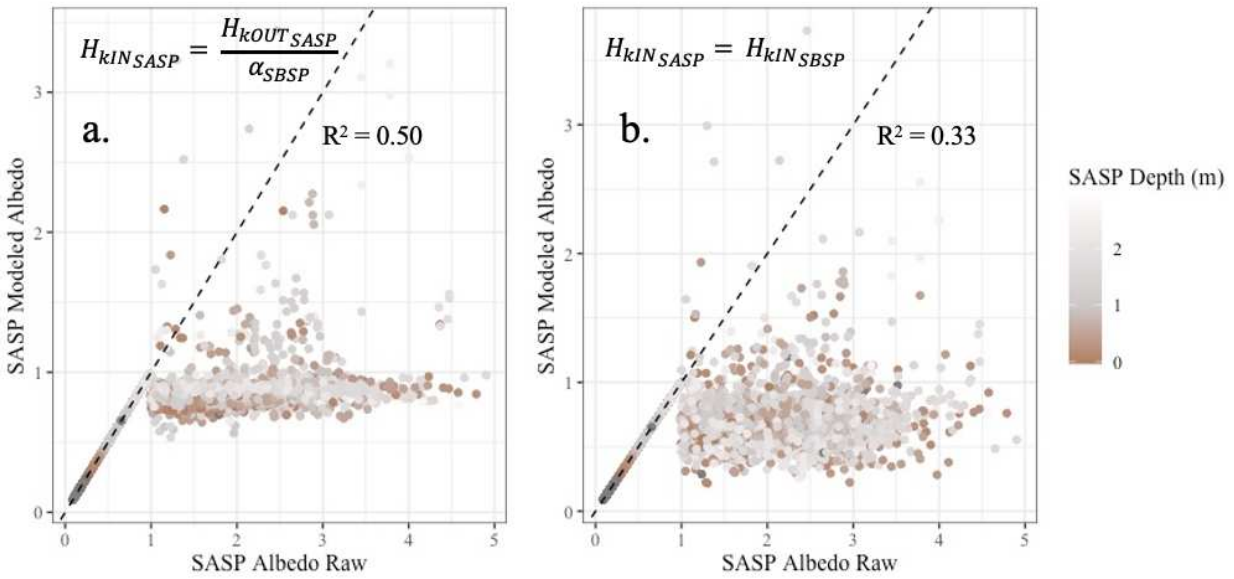
after LaChapelle (1961).

$$\rho_{s_{freshHedstrom-Pomeroy}} = 67.92 + 51.25 * e^{\left(\frac{T_a}{2.59}\right)} \quad [A-5],$$

after Hedstrom and Pomeroy (1998).

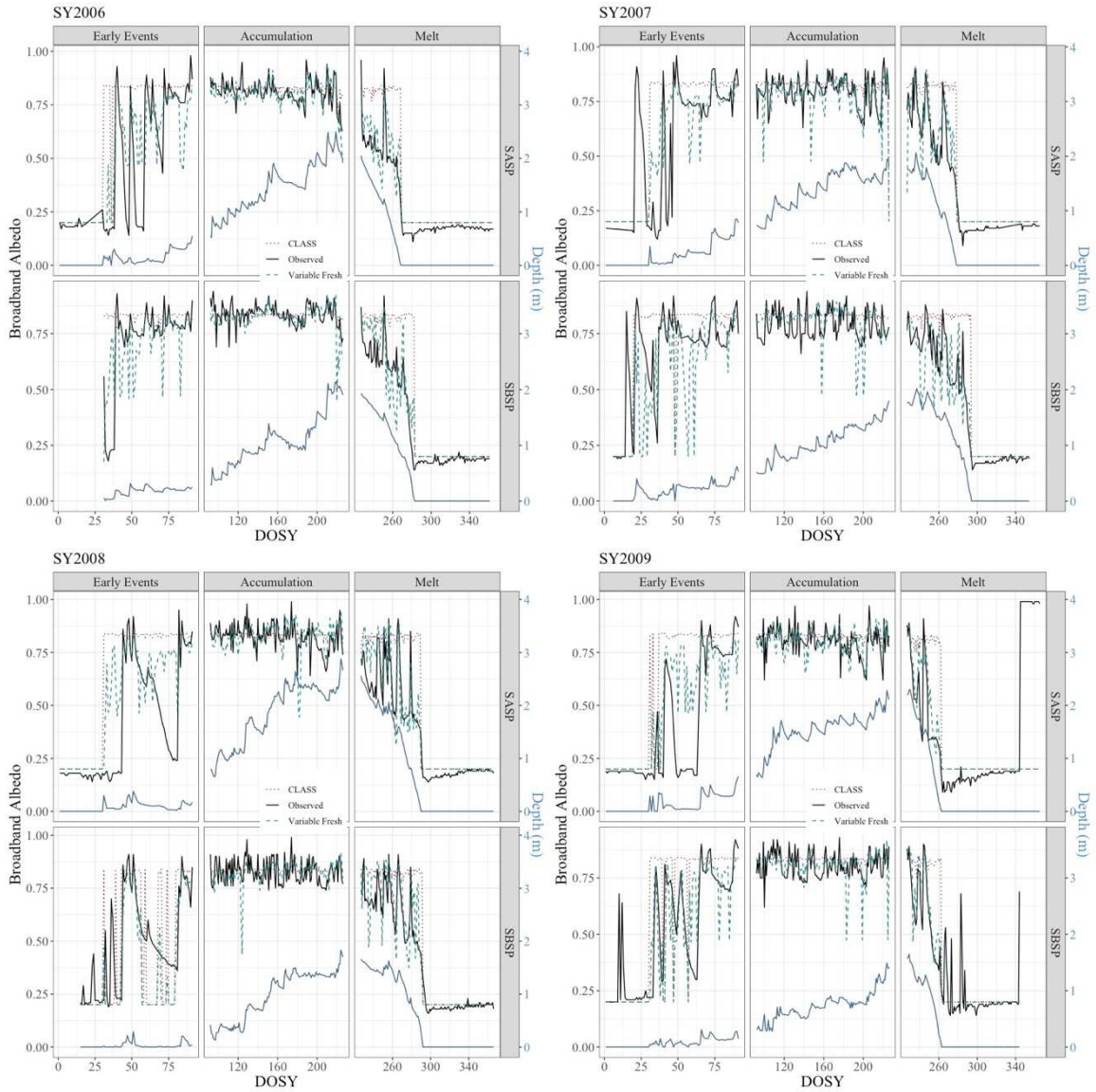
$$\begin{aligned} \rho_{s_{freshparticle\ shape}} = & 85 * [0.030 * \cos(0.331T_a + 0.418) \\ & + 0.015 * \cos(2 * 0.331T_a + 0.418) \\ & - 0.029 * \cos(3 * 0.331T_a + 0.418) \\ & + 0.123 * \sin(0.331T_a + 0.418) \\ & + 0.009 * \sin(2 * 0.331T_a + 0.418) \\ & - 0.026 * \sin(3 * 0.331T_a + 0.418)] * 1.75 + 1] \end{aligned} \quad [A-6],$$

after Fassnacht and Soulis (2002).



**Figure A-1.** Modeled albedo at SASP using observed albedo from SBSP (a) and modeled albedo at SASP using observed incoming shortwave radiation at SBSP (b). A stronger correlation is seen in figure (a) than (b), showing improvements using albedo values from SBSP rather than incoming shortwave radiation values from SBSP.

## APPENDIX B. INDIVIDUAL SNOW YEAR RESULTS



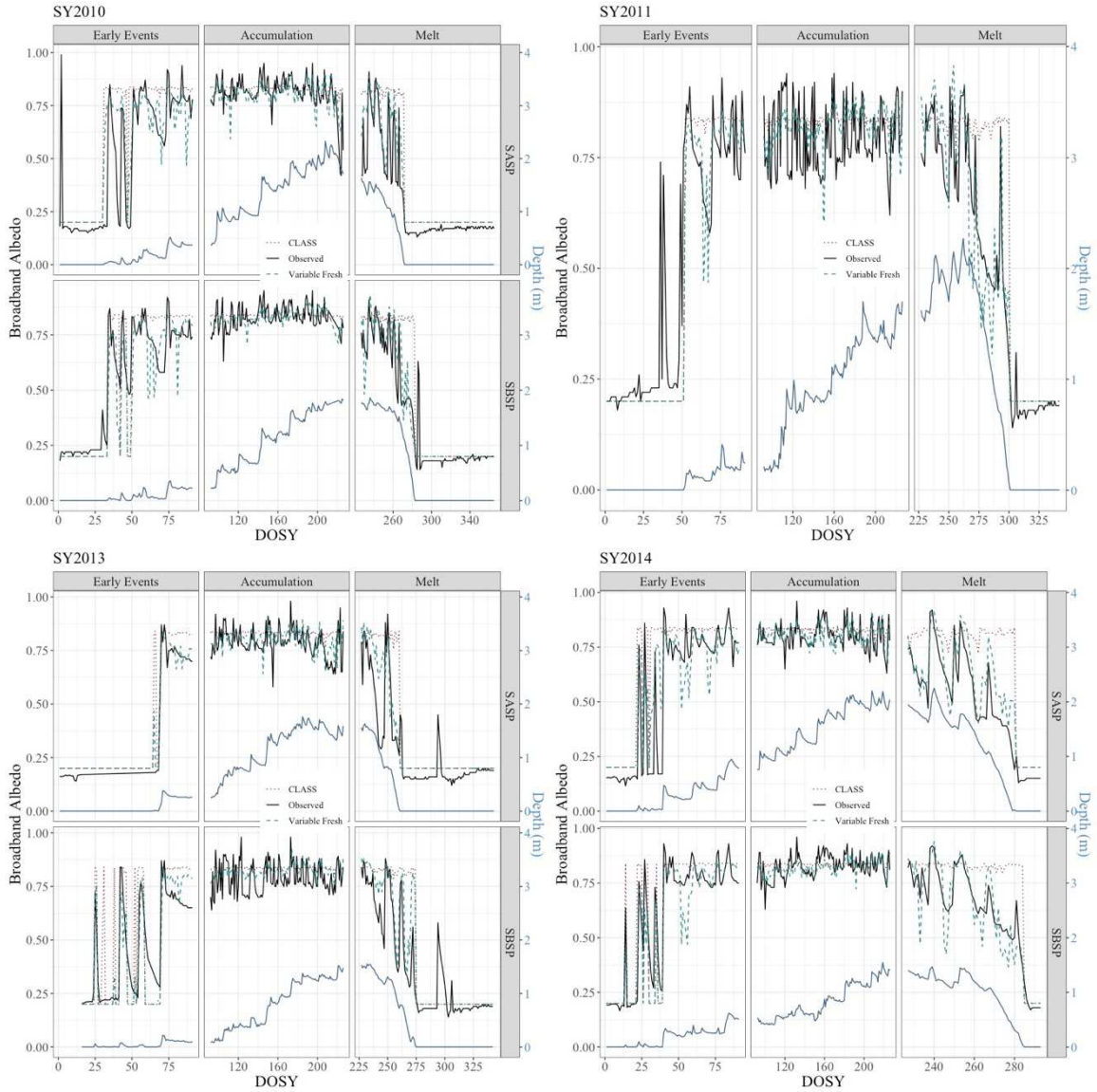


**Figure B-1.** Mean daily observed, Variable Fresh modeled, and CLASS modeled broadband albedo and depth for eight individual snow-year at Swamp Angel and Senator Beck Study Plots. Each year shows similar characteristics in albedo between different seasonal periods. SY2011 only shows results for SBSP.

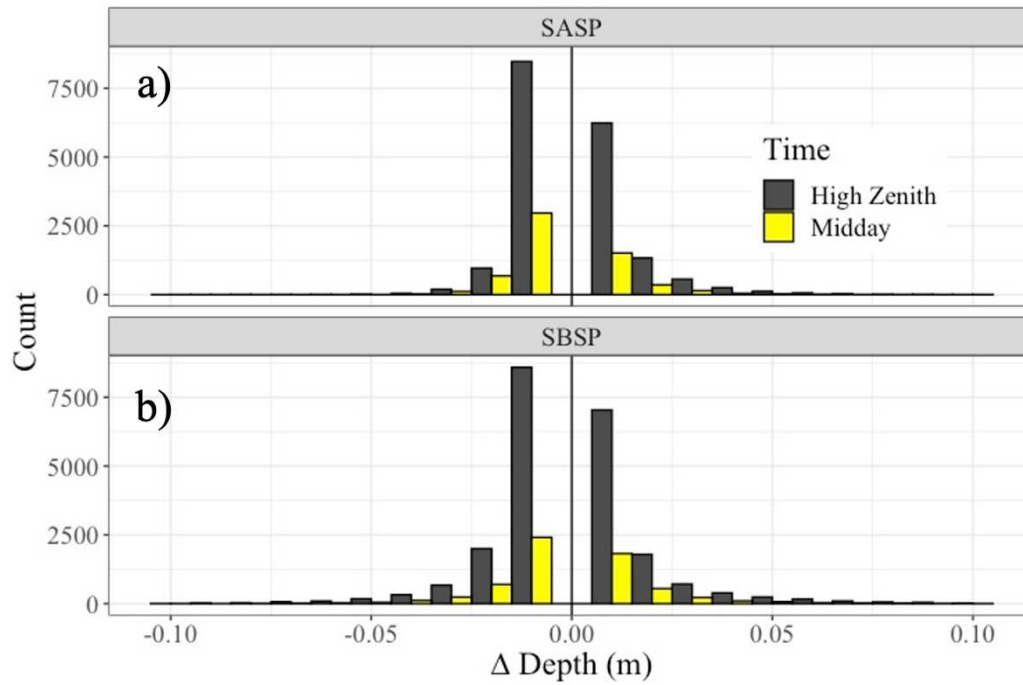


**Figure B-2.** Histogram comparing changes in snow depth per hour between hours where measures albedo is reliable (Midday; +/- 2 hours from solar noon) versus hours that albedo is uncertain (High Zenith; other hours) at the Swamp Angel (a) and Senator Beck (b) Study Plots.

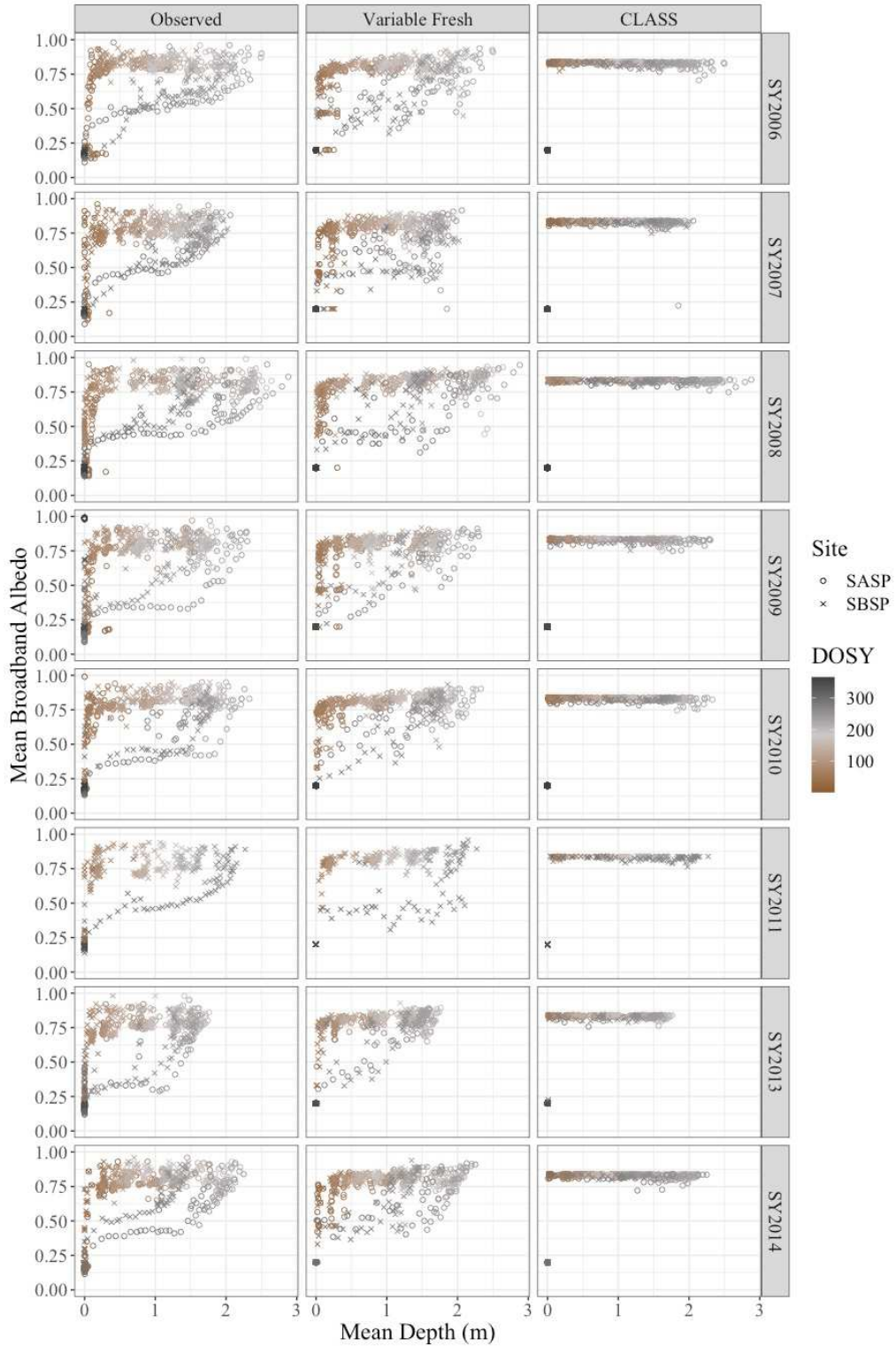


**Figure B-3.** Solar noon depth plotted against solar noon broadband albedo per day for observed values, the variable fresh snow model, and CLASS model for all snow years. Colored by the day (September 1 = DOSY1 and August 31 = DOSY365) separating Swamp Angel (SASP) and Senator Beck Study Plot (SBSP).

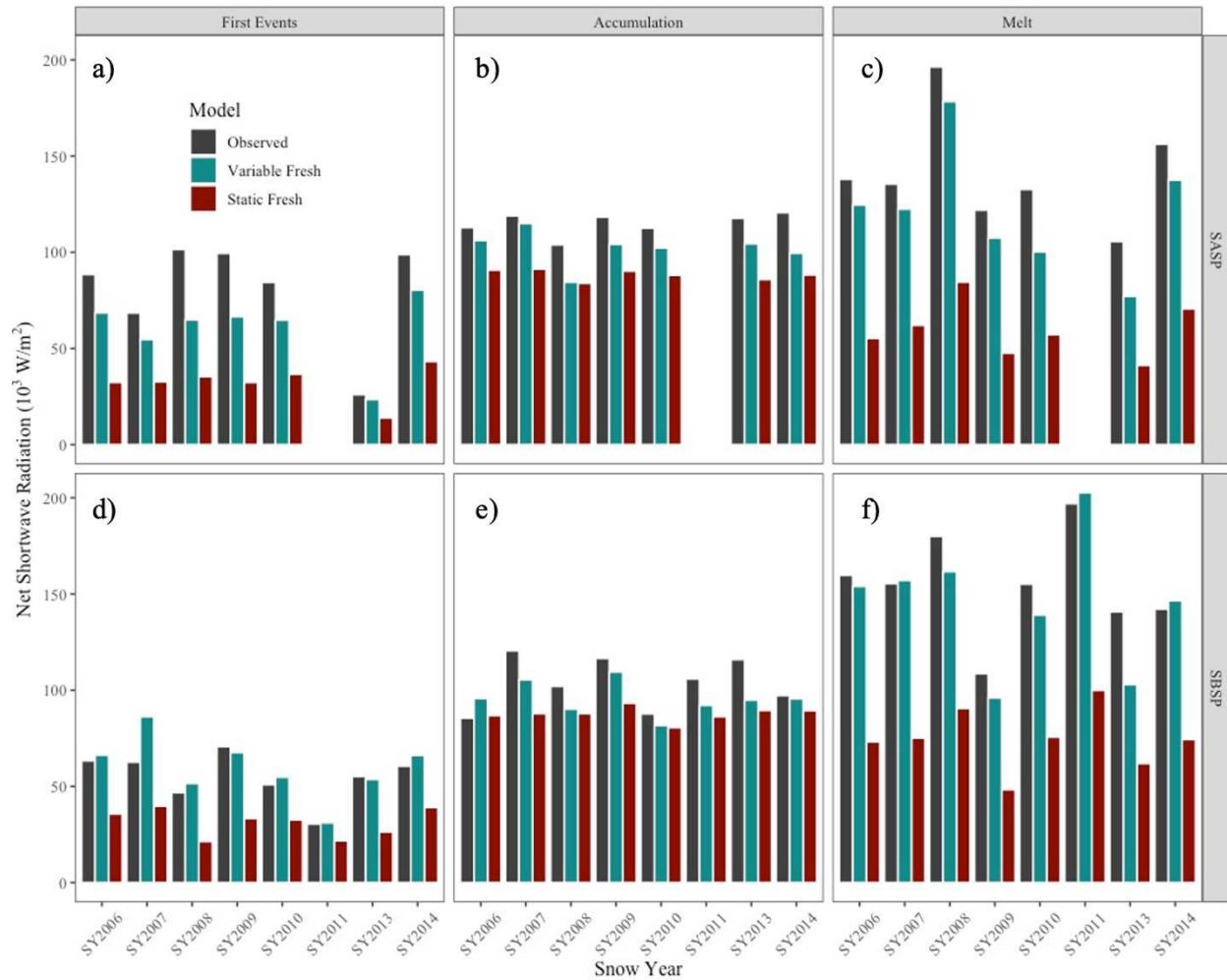


**Figure B-4.** Absorbed shortwave radiation for each snow year during three time frames of the snow season for two sites, SASP and SBSP. The Variable Fresh Snow model outperforms the CLASS Static Fresh Snow model when compared to observed absorption values, especially during times of melt when all observed values are greatest.

APPENDIX C. MULTIVARIATE REGRESSION

**Table C-1.** Cross Correlation ( $R^2$ ) between the variables within the multivariate regression

	Depth	$\Delta$ Depth	Temperature	Albedo (t-1)	# Of Dust Events
Depth	1	0.0012	0.0115	0.1075	0.1504
$\Delta$ Depth		1	0.0116	0.0144	4.273e-07
Temperature			1	0.2469	0.0628
Albedo (t-1)				1	0.0077
# Of Dust Events					1

**Table C-2.** Covariance between the variable within the multivariate regression

	Depth	$\Delta$ Depth	Temperature	Albedo (t-1)	# Of Dust Events
Depth	0.3448	0.0004	-0.3877	0.0246	0.4935
$\Delta$ Depth		0.0004	-0.0129	0.0003	-2.772e-05
Temperature			37.8279	-0.3899	3.3403
Albedo (t-1)				0.0163	-0.0243
# Of Dust Events					4.6956